Master Food Safety
Master's Thesis
TOX80436

Non-specific plastic binding and permeability characteristics of prenylated (iso)flavonoids in *in vitro* Caco-2 cell permeability assay

Yifan Wang[a,1,*], Janniek Ritsema[b,1,2], Nynke Kramer[c,1]

[a]*MSc student in Master Food Safety*
[b]*Daily supervisor*
[c]*Thesis examiner*
[1]*Toxicology Chair Group, Wageningen University, P.O. Box 8000, 6700 EA Wageningen, The Netherlands*
[2]*Food Chemistry Chair Group, Wageningen University, P.O. Box 17, 6700 AA Wageningen, The Netherlands*

Abstract

Prenylated (iso)flavonoids are derivatives of (iso)flavonoids with higher lipophilicity and have the potential to exhibit higher bioavailability. Analysis of their intestinal absorption through the *in vitro* Caco-2 cell permeability model is challenging due to the potential non-specific binding caused by high lipophilicity. In this study, the suitability of Caco-2 cell permeability assay with 14% (*w/v*) bovine serum albumin (BSA) and the permeability characteristics of non-prenylated genistein and prenylated lupiwighteone, wighteone, and 6,8-diprenylgenistein were investigated by conducting permeability assay with or without Caco-2 cells using reversed-phase ultra-high performance liquid chromatography with photodiode array detection and mass spectrometry (RP-UHPLC-PDA-MS) analysis. By creating a concentration-time profile, it was possible to determine the percentage of wighteone in different compartments at different time points and provide information about the non-specific binding process. The results showed that around 53%, 49% and 50% of lupiwighteone, wighteone and 6,8-diprenylgenistein were bound to the plastic plate and the addition of BSA did not show significant influence. The main process of this non-specific binding is the transfer of compounds from the solution to the plate surface within the first 10 minutes. Slow transfer from surface to inner layer lasted for at least 3 hours. Prenylated (iso)flavonoids did not exhibit higher permeability as expected. This research showed that the high lipophilicity of prenylated (iso)flavonoids may limit both their *in vitro* analysis and their intestinal absorption. Modelling the sample distribution in plate, free medium and cell monolayers could help describe their permeability characteristics more accurately.
Keywords: Prenylated (iso)flavonoids; Caco-2 cell permeability assay; non-specific binding.

1. Introduction

Abbreviations

6,8-DPG	6,8-Diprenylgenstein	AP chamber	apical chamber
BL chamber	basolateral chamber	BSA	bovine serum albumin
Papp	apparent permeability coefficients	SARs	structure-activity relationships
RP-UHPLC-PDA-MS	reversed-phase ultra-high performance liquid chromatography with photodiode array detection and mass spectrometry		

* Corresponding author.
E-mail address: willa.wang@wur.nl
Submission date: 29-2-2024
ECTS: 36 ECTs
Word count: 7067 words excl. acknowledgement, appendix and references

1.1. (Iso) flavonoids and prenylated (iso)flavonoids

Flavonoids are a group of polyphenolic compounds produced by plants and widely present in plant-based food. Their basic 15-carbon skeleton consists of two benzene rings and one heterocyclic pyran ring as shown in **Fig. 1**. Isoflavonoids are the isomeric form of flavonoids and have a phenyl ring (the *B*-ring) at the *C*3 position instead of the *C*2 position (Han et al., 2009). Based on the degree of oxidation of *C*-ring, (iso)flavonoids can be further divided into different subclasses, including flavonols, flavones, isoflavones, anthocyanidins, flavonones, flavanols, and chalcones. In addition, the presence of substituent groups increases the complexity and diversity of (iso)flavonoid groups, including various hydroxyl, methoxyl, methyl, or glycosyl substitution patterns (Shen et al., 2022). Studies showed that (iso)flavonoids have beneficial functions like anti-inflammatory, anti-bacterial ability, and anti-oxidation (Shen et al., 2022). It has also been proved that (iso)flavonoids have certain cytotoxic anticancer properties and can help reduce the risks of multiple cancers (de Souza et al., 2022).

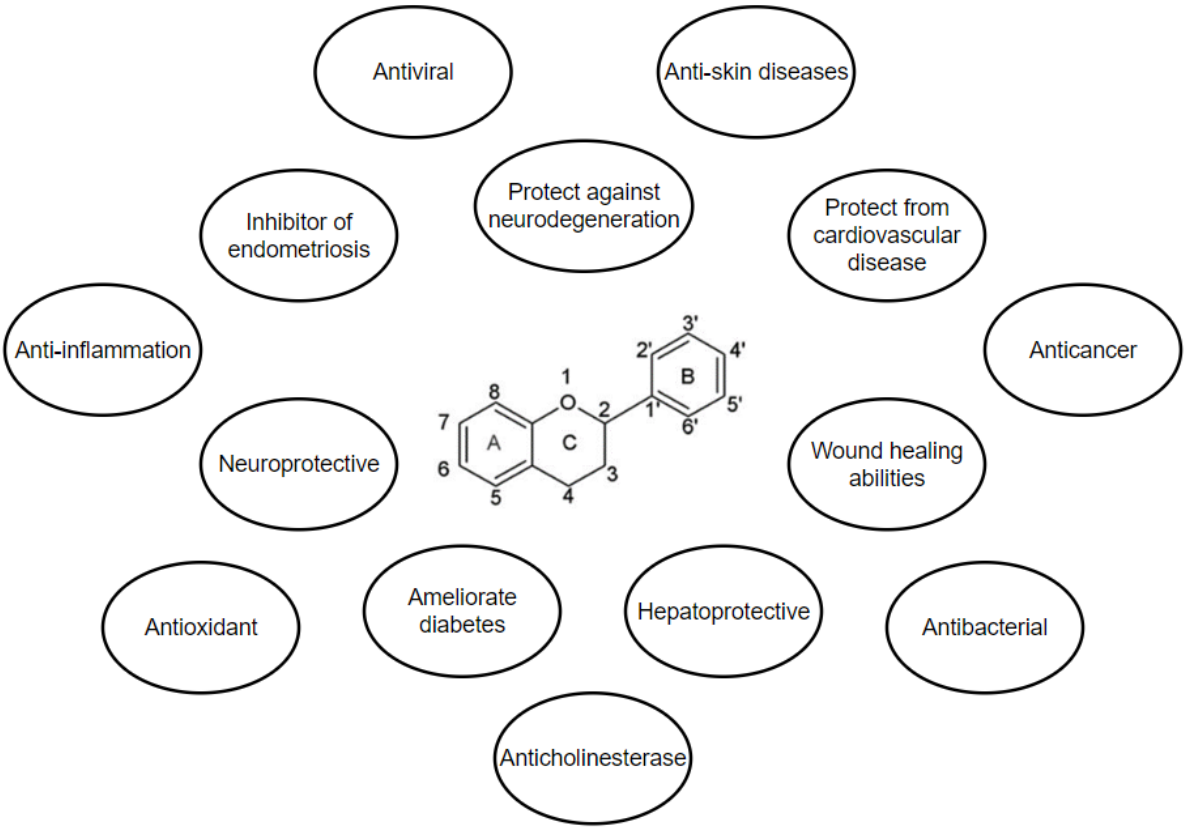

Fig. 1. Basic skeleton and functions of flavonoids (Based on the researches by Ma and Khachemoune (2023), Panche et al. (2016), and Safe et al. (2021))

Prenylated (iso)flavonoids are the derivatives of (iso)flavonoids with lipophilic prenyl side-chain(s) in the (iso)flavonoid skeleton (Shi et al., 2021). In general, *C*-prenylation on flavonoids is more common than *O*-prenylation and *C*-prenylation usually occurs on ring *A* at *C*-6/*C*-8 or ring *B* at *C*-3′/*C*-5′ (Barron & Ibrahim, 1996; Yang et al., 2015). Prenylation increases lipophilicity, affinity to biological membranes, and interaction with target proteins, such as P-glycoprotein in biological membranes (Xu et al., 2012). Kalli et al. (2022) stated that wighteone and glabridin showed antifungal properties against *Z. parabailii* with a distinct mode of action (fast membrane permeabilization) compared to traditional food preservatives. Morachalcone D in mulberry leaf was related to the prevention of ROS production, glutathione depletion, and iron accumulation, which has the potential to be used as a neuroprotective agent in functional food (Wen et al., 2020). Some of their glycosylated forms have also been proved to show anti-inflammatory effects in *in vitro* assay (Zulfiqar et al., 2017).

Even though prenylated or non-prenylated (iso)flavonoids are usually considered non-toxic, some researchers still showed potential toxicity at high doses. Flavonoid quercetin could induce hepatotoxic stress and influence

several genes at doses of 1500 and 2000 mg/kg (Singh et al., 2022). Flavonoid-enriched fractions from *Parastrephia lucida* showed no toxicity or genotoxicity while some of their hepatic metabolic products could be considered genotoxic (D'Almeida et al., 2020). The flavonoid-rich fraction of *Croton blanchetianus Baill* was not genotoxic and its acute oral LD_{50} was determined as > 5000 mg/kg, while the long-term dose of 1000 mg/kg was not suggested due to subacute toxicity (de Oliveira et al., 2022). Prenylated (iso)flavonoids were found to perform selective cytotoxicity against various cancer cells, however, previous evidence showed that they are usually safe to consume and non-toxic to normal cells (Lv et al., 2023; Tronina et al., 2023; Yang et al., 2015).

1.2. Metabolism of (iso)flavonoids and prenylated (iso)flavonoids

The applications of (iso)flavonoids are still limited due to their low bioavailability (Thilakarathna & Rupasinghe, 2013). As shown in **Fig. 2**, (iso)flavonoids usually exist in glycoside forms in plants and some of them could be hydrolysed in the small intestine by lactase-phlorizin hydrolase (LPH), cytosolic β-glucosidase (CBG) and other enzymes to produce aglycons (Day et al., 2000). These aglycons are more easily absorbed and could be metabolized by the intestinal phase II enzymes (*e.g.* UGTs) and phase I enzymes (*e.g.* cytochromes P450) (Chen et al., 2014; Spencer, 2003). Their metabolites will further be transported to the liver and arrive at the other organs or tissues where they work. However, most of the glycosylated (iso)flavonoids will reach the colon unabsorbed and be metabolized by intestinal flora. With regards to the absorption methods, Ahmed et al. (2020) showed that aglycons like quercetin could be absorbed by passive diffusion and some glycosylated (iso)flavonoids may be actively transported by sugar transporters in the Caco-2 cells. However, the permeability and absorption of specific dietary (iso)flavonoids have not been uniformly concluded. Murota et al. (2018) stated that genistein and daidzein can be easily hydrolysed by LPH and absorbed in the intestinal lumen while another research pointed out that almost all isoflavones including genistein and daidzein can reach the colon in glycoside forms without being hydrolysed in small intestine (Magni et al., 2022). These differences may result from their various structures with different amounts and types of linked sugars (Chen et al., 2022).

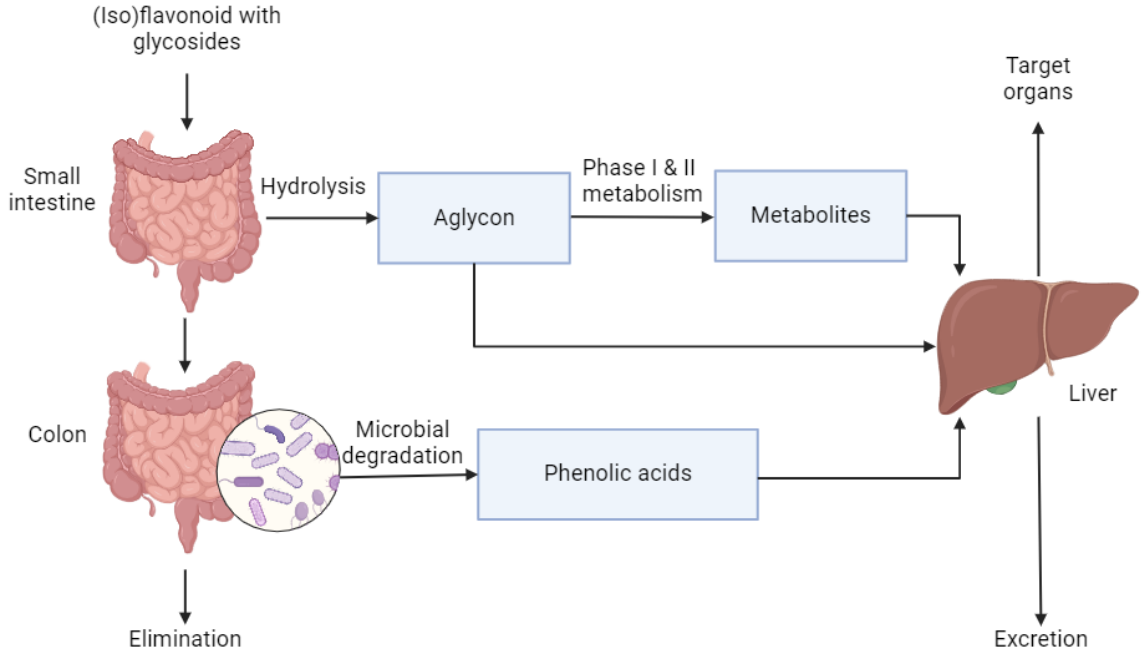

Fig. 2. Metabolic processes of dietary (iso)flavonoids (Based on the researches by Chen et al. (2022) and Murota et al. (2018))

Prenylated (iso)flavonoids have a similar metabolism pathway as non-prenylated (iso)flavonoids but are less abundant in nature (Tao et al., 2017). It was found that some glycosylated prenylated (iso)flavonoids had a low permeability in the Caco-2 cell assay and may be difficult to be absorbed in the intestine (Chen et al., 2008). Therefore, these glycosylated prenylated (iso)flavonoids with a lower cost are usually only used as precursors of non-glycosylated ones instead of being utilized directly (Vongdeth et al., 2018).

1.3. Structure-activity relationships (SARs)

The properties of prenylated (iso)flavonoids are influenced by their chemical structure. In addition to (iso)flavonoid backbone, different prenylation patterns could also make a difference. The amount of prenyl groups is one of the major factors affecting their bioavailability. Compared with the non-prenylated (iso)flavonoids, single prenylated (iso)flavonoids could show higher bioavailability and lipophilicity and therefore increase affinity to hydrophobic biological targets, such as the membrane (Lv et al., 2023; Osorio et al., 2021). Furthermore, single prenylation may increase intestinal uptake and enhance accumulation of (iso)flavonoids in specific tissues (e.g. liver or muscle tissue) by inhibiting efflux compared to non-prenylated (iso)flavonoids (Terao & Mukai, 2014), which may also increase the accumulation in non-target organ and lower the detoxifying elimination. However, research on double-prenylated (iso)flavonoids is still limited. Another factor is the position of prenyl groups. 8-Prenylnaringenin (8-PN) was more bioavailable than 6-prenylnaringenin (6-PN) in an *in vivo* trial (Calvo-Castro et al., 2018). Other than the prenylation amount and position, the structure diversity could also be related to the difference in prenyl group configuration and the presence of other substituted groups like hydroxyl or methoxyl (Kalli et al., 2021). Prenyl groups could occur as chains or by cyclized with adjacent hydroxyl groups to form six-membered rings or five-membered rings (van Dinteren et al., 2021). Liu et al. (2020) stated that the prenylated flavonoids from *Artocarpus heterophyllus* with three hydroxyl groups situated at *C*5, *C*7, and *C*4′ were more active in anti-inflammatory activities with inhibitory effects on nitric oxide production than the ones substituted with methoxy groups.

1.4. Caco-2 cell permeability assay and potential problems

Caco-2 cell permeability assay, based on human colon adenocarcinoma-derived Caco-2 cells, is a commonly used *in vitro* model to study the mechanism of intestinal absorption. These cells can form a monolayer that has similar morphology and functions to the human intestinal epithelial cells (Ding et al., 2016). It can help predict the intestinal absorption of multiple drugs or foods with the advantages of easy culture, passaging, and cryopreservation (Yamada et al., 2023). The results of the Caco-2 cell assay can be expressed as apparent permeability coefficients (Papp) in which a higher Papp value means higher permeability (Ravikanth & Ramanamurthy, 2018).

The permeability in Caco-2 cells has a good correlation with oral absorption in the human body (Angelis & Turco, 2011). However, this model is still not completely applicable for lipophilic and water-insoluble compounds. It is usually difficult to generate effective data due to the low solubility in the assay buffer and/or poor recovery from the assay, non-specific binding to the apparatus (the binding of analytes to non-target molecules on the apparatus), and high monolayer retention (Katneni et al., 2018). Due to the high lipophilicity of prenylated (iso)flavonoids, the solubility and non-specific binding are potential challenges in this research. Therefore, the addition of bovine serum albumin (BSA) was used in this research to optimize the Caco-2 cell permeability assay, which can provide an absorptive driving force and reduce both the non-specific binding and cell association (Krishna et al., 2001).

1.5. Compounds used in the research

To better understand the absorption process of prenylated flavonoids and the influence of prenylation, several compounds from isoflavones groups were selected based on their structural similarity and difference in antimicrobial activity (**Table 1**). Genistein is one of the most widely known and used non-prenylated (iso)flavonoids because of its therapeutic potential in cancer, diabetes, cardiovascular, and neurodegenerative diseases (Drennen et al., 2018). Wighteone and lupiwighteone are *C*-prenylated derivatives of genistein, prenylated at *C*6 and *C*8 positions, respectively. 6,8-Diprenylgenistein (6,8-DPG), a double *C*-prenylated derivative of genistein, has anti-tumour, anti-inflammatory, and anti-obesity properties (Bae et al., 2021). Among these prenylated (iso)flavonoids, 6,8-DPG exhibited effective anti-microbial activity with the lowest concentration, while there was still no anti-bacterial activity of lupiwighteone detected at the concentration of 100 µg/mL (Kalli et al., 2021). Propranolol was selected positive control, as it is completely orally bioavailable and exhibits a Papp value higher than 20×10^{-6} cm/s (Ahmed et al., 2020). According to the previous research, the toxicity of single prenylated (iso)flavonoids glabridin, licochalcone A, and glycycoumarin on Caco-2 cells appeared at the concentrations of 154 µM, 148 µM, and 136 µM, respectively (van Dinteren et al., 2022). Therefore, the concentration of 100 µM was used to avoid cytotoxicity in permeability assay.

Table 1: Structure of the compounds used and their anti-bacterial activity against methicillin-resistant *Staphylococcus aureus*

Structure	Name	Minimum inhibitory concentration (μg/mL)
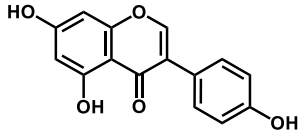	Genistein	> 128 (Choi et al., 2018)
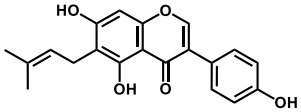	Wighteone	16 (Kalli et al., 2021)
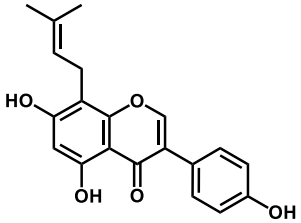	Lupiwighteone	> 100 (Kalli et al., 2021)
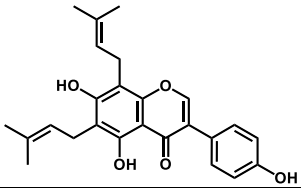	6,8-Diprenylgenistein	9 (Kalli et al., 2021)

1.6. The research purpose, content, and technical route

Prenylated (iso)flavonoids have the potential to be used as innovative medicines and functional ingredients in food. Since prenylated (iso)flavonoids have many structural possibilities due to variations of substituted groups and substituted positions, it is necessary to characterize their toxicity, biotransformation mechanism, and structure-activity relationships (SARs) for better application and safe consumption. Studies have already shown that some single prenylated (iso)flavonoids have the potential to be absorbed with a higher permeability compared to the corresponding non-prenylated (iso)flavonoids. However, the influence of the amount and position of prenyl groups on bioavailability is still unclear. In addition, due to the higher lipophilicity, the application of *in vitro* Caco-2 cell permeability assay may be limited and could not provide effective information.

The overarching goal of this project is to determine the intestinal absorption of several single and double-prenylated (iso)flavonoids. To achieve this goal, the suitability of *in vitro* Caco-2 cell permeability assay with 14% (*w/v*) BSA was evaluated by assessing the solubility, volatility, and non-specific plastic binding of prenylated (iso)flavonoids and creating a concentration-time profile of wighteone. Another aim is to determine their permeability characteristics and the influence of the amount and position of prenyl groups by comparing their Papp values obtained from the Caco-2 cell permeability assay. Reversed-phase ultra-high performance liquid chromatography with photodiode array detection and mass spectrometry (RP-UHPLC-PDA-MS) will be conducted for quantification of prenylated (iso)flavonoids. The technical route is shown in **Fig. 3**. The experiments described in this thesis are based on hypotheses that the Caco-2 cell permeability assay is applicable for hydrophobic prenylated (iso)flavonoids after adding 14% (*w/v*) BSA and prenylated (iso)flavonoids show higher permeability with increased prenyl groups.

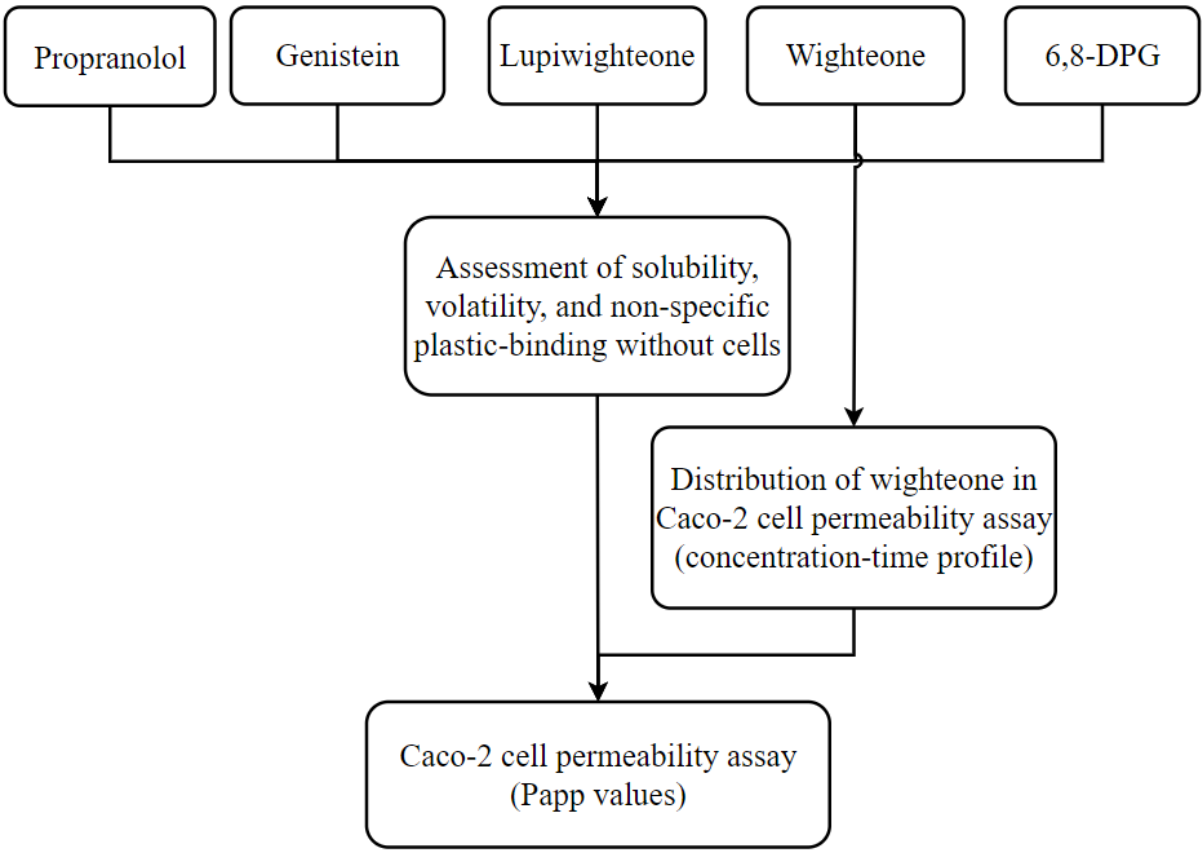

Fig. 3. Technical route of the research

2. Materials and methods

2.1. Materials and apparatus

The information about propranolol, prenylated, and non-prenylated (iso) flavonoid samples used is shown in **Table 2**. For readability purposes, '(prenylated) (iso)flavonoids' is used as the general term to refer to all five compounds, including propranolol. Caco-2 cells were from the common stock in TOX. Culture medium (CM) consisted of 500 mL Minimum Essential Medium (MEM) (Gibco, Thermo-Fisher cat.no21090022) with 20% (*v/v*) Fetal Bovine Serum (FBS, general stock in TOX), 1% (*v/v*) pyruvate (general stock in TOX) and 1% (*v/v*) penicilline/streptomycine/glutamine solution (PSG, general stock in TOX). 500 mL Hank's Balanced Salt Solution (HBSS) solution (1X) (with $CaCl_2$, $MgCl_2$) (Gibco™, Thermo Fisher Scientific Inc., 14025050) with 5 mL 10 mM HEPES (1M) Buffer Solution (Gibco™, Thermo Fisher Scientific Inc., 15630080) was used as the exposure medium (EM). Tissue Culture Inserts for Multiwell Plates (ThinCertTM, 24 wells, 0.4 μm pore sizes, 0.336 cm^2 culture surface, 662640) were purchased from Greiner Bio-One B.V.Cell culture. Other reagents and apparatus are listed in **Table 3**.

Table 2. Information of (prenylated) (iso)flavonoids used

Compound	Concentration of master stock solution (in 100% DMSO, *v/v*)	Purity	Company
Genistein (powder)	-	-	ChemCruz®
Wighteone	20 mg/mL	96%	BioCrick BioTech
Lupiwighteone	10 mg/mL	90%	Unknown
6,8-Diprenylgenistein	20 mg/mL	80%	Plantech U. K
(±)-Propranolol hydrochloride (powder)	-	≥99% (TLC)	Sigma-Aldrich®

Table 3. Reagents and apparatus used

Name	Company
Phosphate buffered Saline (PBS) pH 7.4 (1X)	Gibco™, Thermo Fisher Scientific cat. no.10010015
Bovine Serum Albumin (BSA)	Sigma-Aldrich, CAS no: 9048-46-8
0.25% (*w/v*) Trypsin	General stock in TOX in Wageningen University & Research
Methanol with or without 0.1% formic acid (MeOH, UPLC/MS grade)	Biosolve (Valkenswaard, The Netherlands)
Acetonitrile with or without 0.1% formic acid (ACN, UPLC/MS grade)	Biosolve (Valkenswaard, The Netherlands)
1.5 mL short thread vials	BGB Analytik Benelux B.V., Germany
Chromacol 03-FISV 300 µL fixed insert vial	Thermo Scientific, Germany
SureSTART™ 6PSV9-03FIVP vial	Thermo Scientific, Germany
CELLLSTAR® 24 Well Cell Culture Multiwell Plates	Greiner Bio-One B.V., Cat.-No.662160
Thermo Vanquish UHPLC system	Thermo Scientific, San Jose, CA, USA
LTQ Velos Pro linear ion trap mass spectrometer system	Thermo Scientific
Z 323 High-Performance Centrifuge	Hermle
XP6 Micro Balance	©METTLER TOLEDO
EVOM2™ Epithelial Voltohmmeter	World Precision Instruments
Cellometer® Auto T4 Plus Cell Counter	Nexcelom Bioscience LLC, USA, Serial Number: Auto T4-203-0430

2.2. Sample preparation

The master stock solutions and powder were diluted or dissolved to 20000 µM in 100% (*v/v*) DMSO as working stock solutions. A detailed dilution plan is shown in *Appendix A.1*. Solution with a concentration of 100 µM (0.5% DMSO, *v/v*) was used for permeability assay by diluting the working stock solution (200x) with the exposure medium. A mixture solution was made by mixing 5 µL of each stock solution and diluting it with 975 µL exposure medium (100 µM for each compound, 2.5% DMSO, *v/v*) for the assessments without cells and calibration curves.

2.3. Caco-2 cell sub-culturing and seeding

Caco-2 cells in the flask with confluency <70% needed to be subcultured to avoid differentiation. The CM in the flask was pipetted and the dead cells and serum were removed by washing with 6 mL PBS twice. Then detachment was achieved by being covered with 2 mL of 0.25% (*w/v*) trypsin for approximately 10 seconds. After removing 1 mL of trypsin, the flask was incubated at 37 ℃ for 5 minutes. Another 5 mL CM was added to resuspend the cells. Cell suspension was collected and pipetted up and down to separate cell clusters. For each sub-subculturing, 2 mL cell suspension was kept and mixed with another 8 mL CM as the new generation. Caco-2 cells were placed

in the CO_2 incubator at 37 ℃ until the confluency was around 50-60%.

For further permeability assay, Caco-2 cells (passage numbers 5-12) were seeded onto transwell plates at a density of 2 $\times 10^5$ cells/cm^2. Two flasks of Caco-2 cells in the same generation were detached with the same procedure of sub-culturing and mixed with 5 mL CM. Cell suspension was counted by auto cell counter and diluted to achieve the concentration of 3.36 $*10^5$ cells/mL for 24-well transwell plate (0.336 cm^2) seeding. For the 24-well plate, only the 12 wells in the middle lines were used due to the edge effects. Cell suspension (200 µL) and CM (600 µL) were added to the apical (AP) and basolateral (BL) chambers, respectively. The 24-well transwell was incubated plate at 37 ℃ and the CM was refreshed every 2-3 days (100 µL in the AP chamber and 600 µL in the BL chamber) until the late confluence (21 days).

2.4. Assessment of volatility, apparatus affinity, and BSA extraction efficiency by adding ACN/MeOH

Mixture solution with a volume of 100 µL was added to glass vials and placed in the water bath (37 ℃) with the lid open for 1 hour to assess the volatility. To assess the efficiency of extraction of BSA by organic solvent, 100 µL mixture solution was mixed with 600 µL EM with 14% (*w/v*) BSA. Then 20 µL solution was sampled and mixed with 80 µL MeOH or ACN and shaken for 2 hours. Sample solution (50 µL) from each assessment was detected by RP-UHPLC-PDA-MS after centrifugation at 9000 *g* for 5 min. These assessments were conducted in technical duplicates. To better understand the properties of (prenylated) (iso)flavonoids, related distribution coefficient (logD), ionization, and aqueous solubility (logS) at pH of 7.4 were calculated using MarvinSketch 23.17.

In the plastic-binding affinity assessment, the 24-well transwell plate without cells was used. Mixture solution (100 µL) and EM (600 µL) were added to the AP chambers and the BL chambers, respectively, and the plate was placed in the incubator (37 ℃) for 2 hours. The sample solution (50 µL) from the BL chamber was detected by RP-UHPLC-PDA-MS after centrifugation at 9000 *g* for 5 min. As a comparative group, 100 µL mixture solution and 600 µL EM with 14% (*w/v*) BSA were added to AP and BL chambers in another well. After 2 hours, 20 µL solution from BL chamber was sampled and mixed with 80 µL MeOH for BSA extraction. Then 50 µL sample solutions were detected by RP-UHPLC-PDA-MS after centrifugation at 9000 *g* for 5 min. Another 100 µL and 600 µL MeOH were added to the AP and BL chambers after all liquid was aspired from the plate used to extract the (prenylated) (iso)flavonoids bound to plastic. Sample solution (50 µL) was taken from each well after 2 hours of shaking and then centrifuged at 9000 *g* for 5 min for RP-UHPLC-PDA-MS analysis. This assessment was performed in technical triplicate.

2.5. Caco-2 cell permeability assay

The CM in seeded plates were removed and prewarmed EM was added for 30 min at 37 ℃ (100 µL in the apical chamber and 600 µL in the basolateral chamber). The transepithelial electrical resistance (TEER) value of Caco-2 cell monolayers in EM was measured before the permeability assay, where a TEER value above 300 Ω.cm^2 can indicate good integrity. EM with 14% (*w/v*) BSA (600 µL) was added to all basolateral chambers after aspirating all EM from the plate. Genistein, lupiwighteone, wighteone, 6,8-DPG, or propranolol solutions at the concentration of 100 µM and volume of 100 µL (in EM with 0.5% DMSO, *v/v*) were added to the apical chambers.

The sample solutions (2 µL) were taken from each apical chamber immediately (in 2 min) to correct the initial concentration and mixed with 48 µL MeOH. At the time points 10, 30, 60,120, and 180 min, 10 µL solutions in the basolateral chambers were removed and replaced with 10 µL fresh EM with 14% (*w/v*) BSA. Then 40 µL MeOH was added to each sample solution. Another 10 µL solutions were taken from each apical chamber at 180 min and mixed with 40 µL MeOH.

After the permeability assay, the liquid in the plate was removed and EM was added again (100 µL in the apical chamber and 600 µL in the basolateral chamber). The TEER values were measured again to confirm whether (prenylated) (iso)flavonoids performed significant toxicity to Caco-2 cells and the EM was removed. Then the inserts were moved to new wells. MeOH was added to the used wells (600 µL) and new wells with used inserts (100 µL in the apical chamber and 600 µL in the basolateral chamber) to extract the samples bound to the plate. Sample solutions (50 µL) were taken after shaking the plate (covered with parafilm) at 37 ℃ for 1~2 hours. All sample solutions were shaken for better extraction and stored in the freezer until the supernatant (after centrifugation at 9000 *g* for 5 min) was detected by RP-UHPLC-PDA-MS. The assay was carried out in technical duplicate.

The Papp expressed in centimetres per second (cm/s) were calculated by the equation (Daruhazi et al., 2013)：

$$Papp = \frac{\frac{dC}{dt} \times V_R}{A \times C_0} \quad (1)$$

In which V_R is the volume of medium in the basolateral chamber (600 µL); dC/dt is the slope of the curve based on concentration changes of samples in the basolateral chamber over time (seconds); A is the area of membrane surface area (0.336 cm^2); and C_0 is the initial concentration in the apical chamber.

2.6. The distribution of wighteone in the different compartments (concentration-time profile)

The TEER values were measured as described above and 600 µL EM with 14% (*w/v*) BSA were added to all basolateral chambers. Wighteone solutions (100 µL 100 µM in EM with 0.5% DMSO, *v/v*) were added to all apical chambers. Each well was designed to show the distribution of wighteone at one of the timepoints of 0, 10, 30, 60, 120, and 180 min. Caco-2 cell permeability assay was conducted in all wells and stopped at the corresponding time for each well. At the corresponding time, 10 µL samples were taken from both apical and basolateral chambers in the corresponding groups and mixed with 40 µL MeOH. The TEER values in EM were measured again and the inserts were moved to a new well after aspiring the EM. When the assay in all wells was finished, MeOH was added to extract samples from both the used inserts and wells (inserts: 100 µL in the apical chamber and 600 µL in the basolateral chamber; wells: 600 µL). The plate (covered with parafilm) was shaken at 37 ℃ for 1~2 hours. All sample solutions were shaken for better extraction and stored in the freezer until the supernatant (after centrifugation at 9000 *g* for 5 min) was detected by RP-UHPLC-PDA-MS. The assay was carried out in technical duplicate.

2.7. RP-UHPLC-PDA-MS analysis

RP-UHPLC-PDA-MS analysis was conducted using a Thermo Scientific - Vanquish / Thermo Scientific - LTQ VelosPro system equipped with a pump, degasser, autosampler, and UV detectors. The analysis was performed on a reversed-phase Acquity UPLC ® BEH C18 column (2.1 × 150 mm, 1.7 µm; Waters Corporation., Part No. 186002353) with a VanGuard (5 mm × 2.1 mm, 1.7 µm) guard column of the same material (Waters, Milford, USA). The column temperature was 45 ℃ and the temperature of the autosampler was 37 ℃. Eluents used consisted of eluent A (water + 0.1% formic acid, *v/v*) and eluent B (acetonitrile + 0.1% formic acid, *v/v*) at a flow rate of 0.4 mL/min. A gradient flowing consisting of 25% eluent B increased linearly to 75% from 1.09-14.72 min as shown in *Appendix B.1*. At 1.09 min the eluent flow was redirected towards the MS. The total run time was 27.80 min. Detection wavelengths for UV absorbance were set at 280 nm with an injection volume of 1 µL. Mass spectrometric data were collected in negative ionization (NI) and positive ionization (PI) mode between *m/z* 200-1000 using an LTQ Velos Pro linear ion trap mass spectrometer (Thermo Scientific) equipped with a heated electrospray ionization (ESI) probe. Data-dependent MS^2 (both NI and PI) and MS^3 (only PI) spectra of multiple different ions present in full MS were obtained at the same time. The retention time, *m/z* and ionization mode of each compound are shown in *Appendix B.3*.

2.8. Data analysis

Data collected by RP-UHPLC-PDA-MS was analysed using Xcalibur Qual 4.1 and GraphPad Prism 10.1.2. The quantification was conducted by comparison of peak area to standard curves of mixture solution. ICIS integration algorithm was used to integrate peaks in mass chromatograms. Only the peaks with a (signal-to-noise ratio) S/N higher than 10 were regarded as reliable and used for calculation. A two-way analysis of variance (ANOVA) was conducted based on the variables and the difference was considered significant when $p<0.05$. Results were expressed as the mean ± standard deviation (SD) for the experiments with triplicates. For the experiments with only duplicates, results were expressed as the mean, and the original data points were involved in the figures.

3. Results

3.1. Physicochemical properties of (prenylated) (iso)flavonoids

A series of assessments without cells were conducted first to obtain more information about the physicochemical properties and non-specific binding of (prenylated) (iso)flavonoids used. Turbidity was observed during the

dilution of prenylated (iso)flavonoids in EM at room temperature and most of the turbidity disappeared after being placed in the water bath. After the volatility assessment (*Appendix D*), the concentration detected in wighteone and lupiwighteone decreased (84.7% and 91.7% remaining, respectively). For propranolol, genistein, and 6,8-DPG, the concentration increased after volatility assessment. The results of related physicochemical parameters calculated by MarvinSketch are shown in **Table 4**. Prenylated (iso)flavonoids have higher logD values at a pH of 7.4 but only the 6,8-DPG show a logD value higher than 3. At pH=7.4, only around 0.1% of prenylated (iso)flavonoids are still in the neutral form. Prenylated (iso)flavonoids also showed lower logS values for both intrinsic solubility and solubility at a pH of 7.4.

Table 4. Physicochemical properties of the compounds used

Compounds	$LogD_{7.4}$	Percentage of the neutral compound at 37 °C, pH=7.4	Aqueous solubility prediction (intrinsic solubility; logS at pH 7.4)
Propranolol	0.73	2.81	-3.70; -1.83
Genistein	2.12	7.97	-2.40; -3.39
Wighteone	2.27	0.10	-4.88; -2.00
Lupiwighteone	2.37	0.13	-4.88; -2.12
6,8-DPG	3.90	0.06	-6.30; -3.21

3.2. BSA extraction efficiency by adding ACN/MeOH and apparatus affinity without cells

The extraction efficiency of (prenylated) (iso)flavonoids from BSA by MeOH and ACN was analysed by two-way ANOVA. The results are shown in **Fig. 4**. Extraction efficiency of both MeOH and ACN were higher than 80% without significant difference. Considering the price and toxicity, MeOH was selected for all the extraction of BSA in following permeability assays.

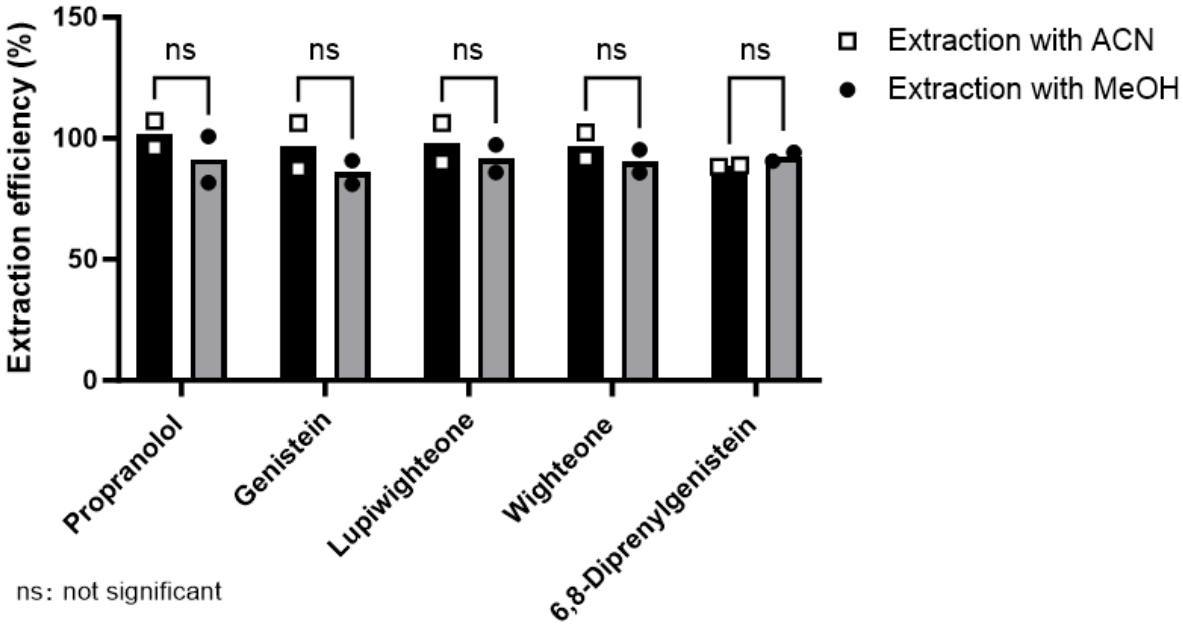

Fig. 4. Extraction efficiency (%) of different compounds from BSA using ACN or MeOH.

The results of apparatus affinity analysed by two-way ANOVA are shown in **Fig. 5** and the distribution of

(prenylated) (iso)flavonoids is shown in **Fig. 6**. More than 70% of genistein and propranolol were still in the free medium while only 27.4 ± 3.4%, 44.8 ± 5.0% and 18.6 ± 8.2% of lupiwighteone, wighteone and 6,8-DPG remained in free medium without adding BSA. The effect of adding BSA on the reduction of plastic-binding effect was also not significant (39.9 ± 10.9%, 46.8 ± 10.6% and 31.6 ± 8.2% for lupiwighteone, wighteone and 6, 8-DPG remained, respectively). The distribution of compounds in different compartments also confirmed that around 50% of wighteone, lupiwighteone and 6,8-DPG were bound to the plastic 24-well plate.

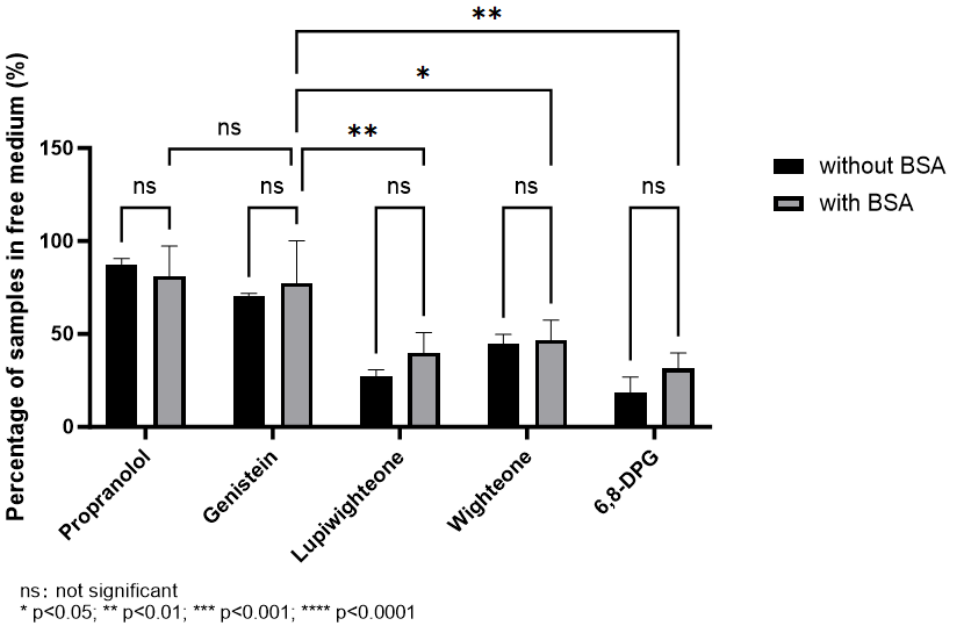

Fig. 5. Plastic-binding affinity of prenylated and non-prenylated (iso)flavonoids and the influence of the addition of BSA

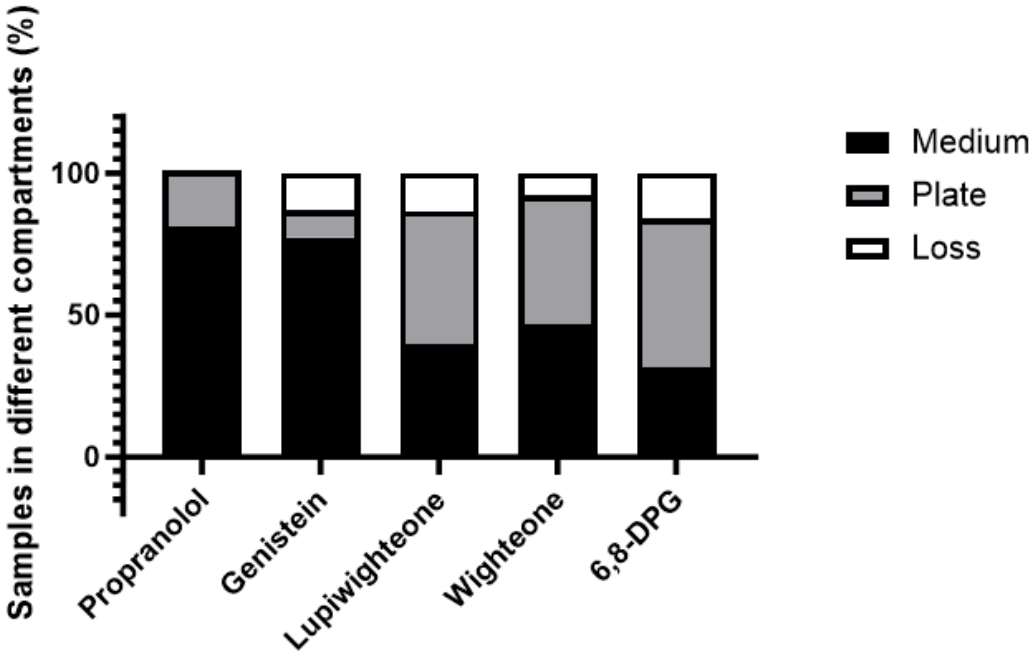

Fig. 6. The percentage of (prenylated) (iso)flavonoids in plate, free medium and loss after adding BSA

3.3. Cell integrity after adding (prenylated) (iso)flavonoids with a concentration of 100 µM

Two-way ANOVA was conducted for the comparison of the changes in TEER values and only the groups with significant differences are annotated in **Fig. 7**. It can be found that TEER values decreased after the permeability assay, especially for the one that lasted for 3h. There was no significant difference between the negative control groups and the experimental groups in both the 2-hour and 3-hour assay, which suggested the decrease of TEER values may be related to the environmental changes or the fluctuation of equipment rather than the toxicity of (prenylated) (iso)flavonoids. In addition, for most of the groups, the TEER values after the permeability assay were still higher than 300 $\Omega.cm^2$, indicating the good integrity of the Caco-2 cell layer.

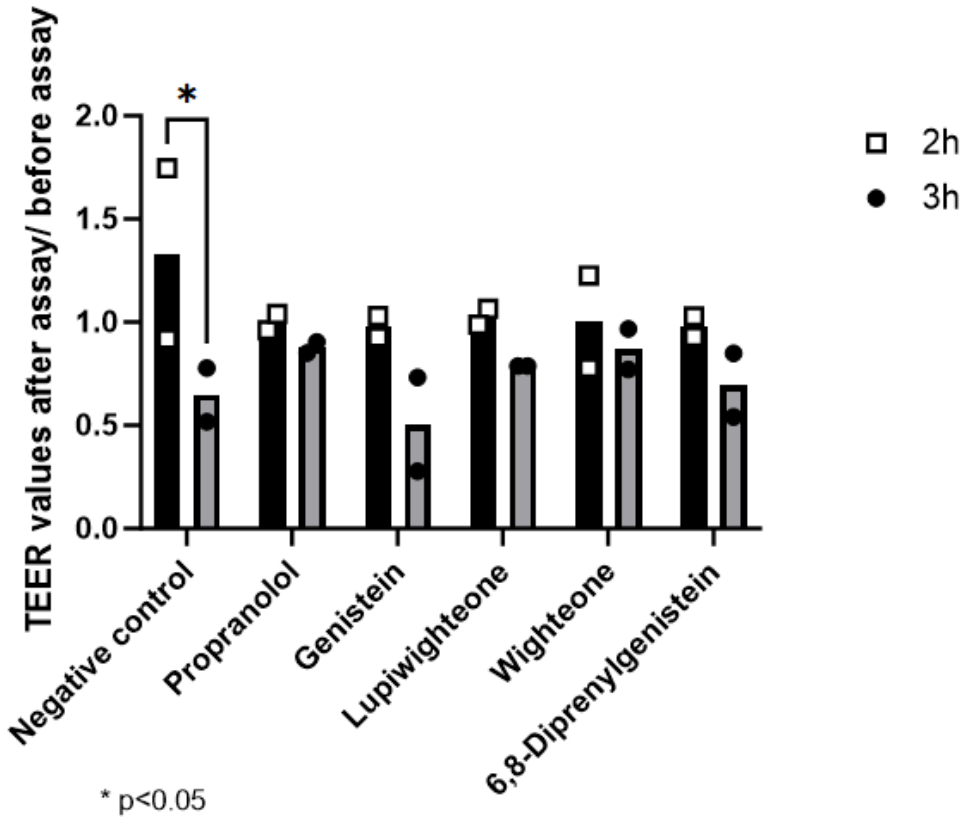

Fig. 7. Changes of TEER values in 2h and 3h Caco-2 cell permeability assay.

3.4. The concentration-time profile of wighteone in the different compartments

The percentage of wighteone distributed in different compartments at different time points is shown in **Fig. 8**. It can be found that the binding occurred at the beginning of the permeability assay and was fastest in the first 10 min. The binding process between the medium in the AP chamber and the plastic plate did not reach the balance until the end of the 3h permeability assay and only 7.17% of wighteone passed the Caco-2 cells.

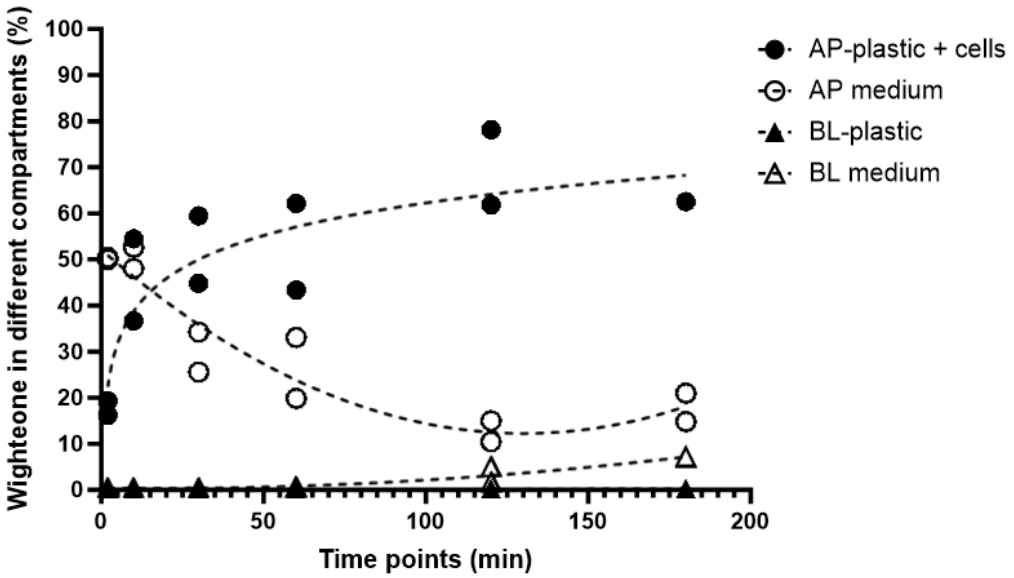

Fig. 8. Distribution of wighteone (%) in Caco-2 cell permeability assay over time. AP-plastic + cells: wighteone bound to the insert and cells, logarithmic regression, Y= 10.19 lnX + 15.39, R^2=0.9032; AP medium: wighteone in free medium in apical chamber, polynomial regression, Y=52.19-0.6131 X+0.002357 X^2, R^2=0.9531; BL-plastic: wighteone bound to wells; BL medium: wighteone in free medium in basolateral chamber, polynomial regression, Y=0.3950-0.006690 X+0.0002485 X^2, R^2=0.9971.

3.5. Caco-2 cell permeability assay

Fig. 9 shows Papp values of different compounds in a 3h permeability assay. The higher Papp values of propranolol (36.07 × 10^{-6} cm/s) and genistein (16.68 × 10^{-6} cm/s) indicated higher permeability. In the 3h assay, the Papp values of lupiwighteone and wighteone were 0.24 × 10^{-6} and 0.27 × 10^{-6} cm/s, respectively. The Papp values of 6,8-DPG could not be calculated since its concentration in the BL chamber is too low to be detected by RP-UHPLC-PDA-MS and therefore not shown in this figure.

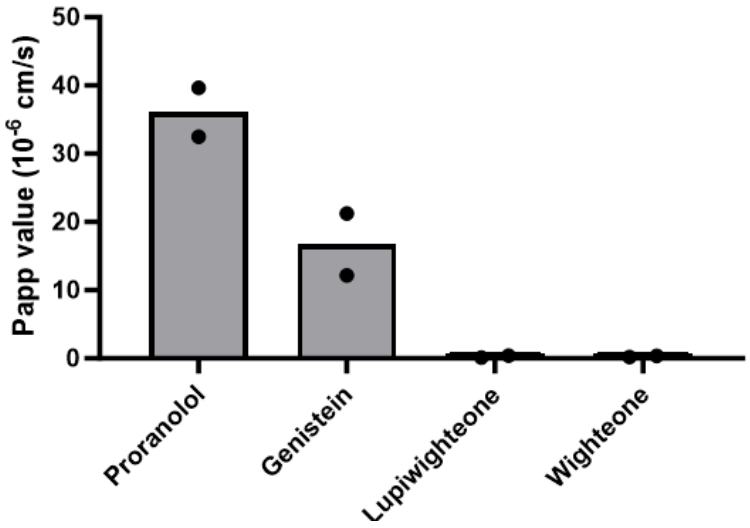

Fig. 9. Papp values of (prenylated) (iso)flavonoids in 3h permeability assay.

Fig. 10 shows the percentage of compounds in different compartments after a 3h Caco-2 cell permeability assay. It was found that 67.43% of propranolol and 43.3% of genistein passed the cells and remained in the medium in the BL chamber. However, 57.39% of lupiwighteone, 47.16% of wighteone, and 77.74% of 6,8-DPG were bound to the plate or cells and most of the rest were still in the medium in the AP chamber instead of passing the Caco-2 cells.

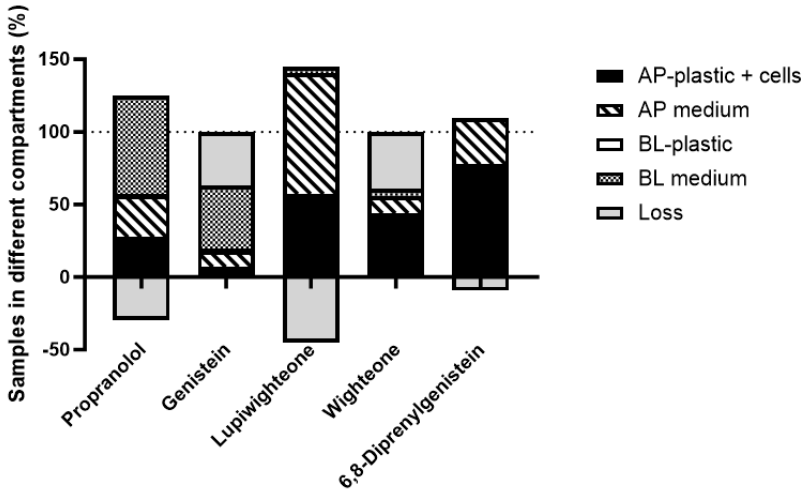

Fig. 10. Distribution of samples (%) at the end of 3h Caco-2 cell permeability assay. AP-plastic + cells: samples bound to the insert and cells; AP medium: samples in free medium in apical chamber; BL-plastic: samples bound to the wells; BL medium: samples in free medium in basolateral chamber; Loss: samples lost during the assay, calculated by (100% - samples in other compartments).

4. Discussion

Prenyl groups have the potential to increase the bioavailability of functional (iso)flavonoids by increasing the hydrophobicity. The increased hydrophobicity could lead to a challenge to *in vitro* Caco-2 cell permeability assay due to non-specific binding and make it difficult to determine their permeability or establish SARs for permeability. Therefore, whether the *in vitro* Caco-2 cell permeability assay is applicable after adding 14% (*w/v*) BSA and whether the amount and position of the prenyl groups make a difference in the permeability of (iso)flavonoids was assessed.

4.1. Physicochemical properties indicated low solubility and potentially poor oral absorption

It was found that prenylated (iso)flavonoids cannot be completely dissolved at room temperature but can be dissolved at 37 ℃. Therefore, the temperature in all assessments and RP-UHPLC-PDA-MS analysis was set at 37 ℃. However, temperature changes were still difficult to eliminate and the potential insolubility problems may influence the results. In volatility assessment, the concentration of wighteone and lupiwighteone calculated by standard curves decreased (*Appendix D*). However, the peak area of these two groups obtained from RP-UHPLC-PDA-MS analysis was higher than that of standard solution (100 µM). Therefore, the decrease of concentration for wighteone and lupiwighteone may be related to the statistical error instead of sample evaporation. The increased concentration of other groups may be due to the evaporation of solvent.

LogD is commonly used to measure the lipophilicity of molecules and relates to the relative ability of crossing cellular membranes (Boldon & Shell, 2023). Higher logD values indicate higher lipophilicity and the optimal range for oral bioavailability is 1-3 (Lindsley, 2014). **Table 4** showed that 6,8-DPG has a low solubility with a $logD_{7.4}$ higher than 3, which suggests poor oral absorption and high plasma protein binding. For other samples with a $logD_{7.4}$ from 0 to 3, they may show good permeability and oral absorption. The low percentage of neutral compounds at the pH of 7.4 indicated that prenylated (iso)flavonoids may not pass the cell membrane since only un-ionized fractions can cross the cell membrane and be utilized by the human body due to the lipid nature of the membrane (Chillistone & Hardman, 2017). Lupiwighteone, wighteone and 6,8-DPG have low intrinsic solubility (<-4). However, at pH = 7.4, their solubility increases with a relatively higher logS.

4.2. Non-specific apparatus binding without adding cells

According to the assessment of apparatus affinity (**Fig. 5**), it was found that for all compounds, including the propranolol, non-specific plastic-binding occurred and resulted in poor recovery of prenylated (iso)flavonoids. This non-specific binding to containers is well-known in the medical field, which is driven by hydrophobic interactions (van der Waals) and ionic interactions (Fukazawa et al., 2010). Hydrophobic interactions with hydrophobic plastic surfaces could be regarded as the main reason for prenylated (iso)flavonoids since they are more hydrophobic and less soluble.

In addition, **Fig. 5** showed the effect of adding BSA is not significant enough to reduce this non-specific interaction even if the binding between (iso)flavonoids and BSA has already been proved (Papadopoulou et al., 2005). This may be explained by the fact that the non-specific binding to plastics is stronger than the binding between BSA and prenylated (iso)flavonoids. Another possible reason is that prenylation may decrease the binding affinity to BSA. It has already been proved that hydroxylation, methoxylation, and glycosylation appearing at different positions could lead to different influences on protein affinity (Tang et al., 2020). Therefore, the prenylation may also play a role in the protein affinity and further influence the performance of BSA on the Caco-2 cell permeability assay.

4.3. The sorption process of wighteone

The concentration-time profile of wighteone (**Fig. 8**) confirmed the results of assessment of non-specific binding without cells (**Fig. 6**). Non-specific binding to plastics did not reach the equilibrium at 3 hours and was most rapid in the first 10 min. Palmgren et al. (2006) studied the kinetics of multiple basic drug sorption to polystyrene surfaces, which found that the loss of basic drugs to polystyrene well plates and modified polystyrene tubes in water was achieved within the first 15 min. The non-specific plastic binding of wighteone could be regarded as sorption as well, which consists of both absorption and adsorption. Adsorption is the process of drugs in solution attached to the surface of the container and absorption is the following process in which drugs enter the inner layer (Dupire et al., 2023). The sorption process is shown in **Fig. 11**. The concentration-time profile in this research suggested that the adsorption of wighteone to the surface of the plate played a major role and happened in the first 10 minutes, after which absorption continued during the timespan of the permeability assay. Therefore, the process happened in Caco-2 cell permeability assay could be summarized as **Fig. 12**. Wighteone was first bound to the plastic insert before reaching the cells. The rest of them arrived and stayed in the cell monolayer instead of passing it. Only a few amounts of wighteone could enter the BL chamber, followed by the plastic binding to the wells.

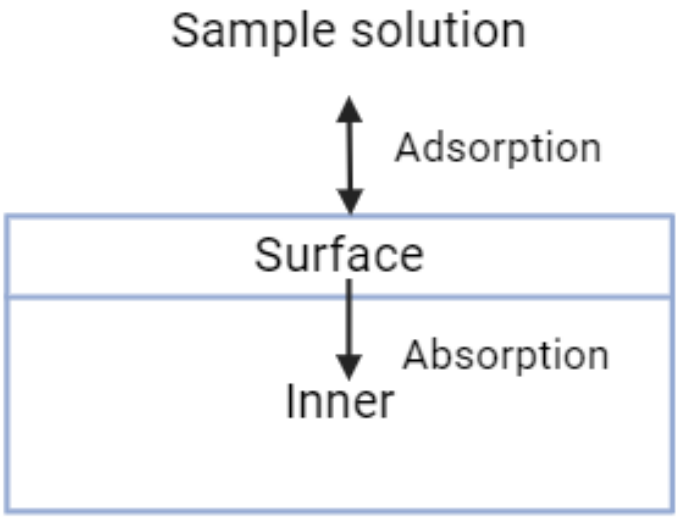

Fig. 11. The process of sorption (based on research by Illum and Bundgaard (1982))

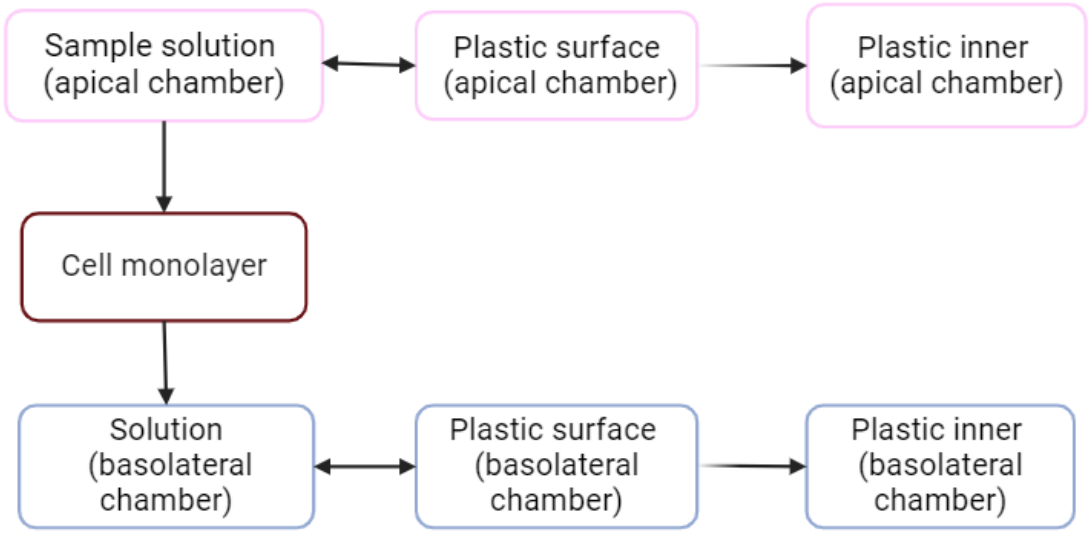

Fig. 12. Process of non-specific binding happened in Caco-2 cell permeability assay

4.4. Comparison of Papp values and permeability

The 2h permeability assay was conducted as well and the results are shown in *Appendix E*, the initial sample concentration was not measured and therefore was assumed to be 100 µM and the Papp values of propranolol (15.18×10^{-6} cm/s) obtained were lower than the reference ($> 20 \times 10^{-6}$ cm/s). It is assumed that (prenylated) (iso)flavonoids may bind to the plate at the beginning (t=0) and then the initial concentration was changed. Therefore, in the 3h permeability assay, the initial sample concentration was corrected based on the detected concentration (C_0) as described in the method.

Due to non-specific binding, the process of permeability assay was influenced and Papp values obtained by the Caco-2 cell permeability assay could not be discussed directly. Even for genistein, the Papp values were also difficult to compare since inconsistent results among different references (ranging from 1.7×10^{-6} cm/s to 50×10^{-6} cm/s) (Daruhazi et al., 2013; Yang et al., 2012). However, it still can be concluded that the permeability of prenylated (iso)flavonoid was not as high as expected compared with genistein since the percentage of prenylated (iso)flavonoids in the BL chamber (both the plastic and medium) were quite low, indicating that most of them did not pass the cells even if they were not bound to the plastic. The low permeability may be related to the low solubility or the fact that most prenylated (iso)flavonoids are ionized and therefore cannot pass the cell layer. The percentage of lupiwighteone and 6,8-DPG bound to inserts in Caco-2 cell permeability assay (57.39% and 77.74%, respectively) were higher than in assessment without cells (46.56% and 48.26%, respectively) (**Fig. 6** and **Fig. 10**). This could be explained by the fact that cell retention or other non-specific reactions may also happen but only to a minor extent.

4.5. Variables in the cell assay and difficulties in quantification

Multiple variables in the cell assay were difficult to be controlled strictly. The different cell lines, culture conditions, passage number, and cell differentiation, could all make a huge difference in the TEER values/monolayer integrity and further influence the results (Kus et al., 2023). In addition to the variability of cells, it is also difficult to standardize the procedure. It is suspected that the 24-well plate may limit the assay since the sample solution may be not mixed evenly in the plate and is difficult to take samples due to the small volume. However, Marino et al. (2005) suggested that the 96-well Caco-2 cell system performed more efficiently than 12-well or 24-well plates. Quantification is also a complicated process for Caco-2 cell permeability assay. The sensitivity of the equipment is a barrier. When using the 24 well plates, the volume sampled was too low for the UHPLC autosampler, and therefore needed to be diluted. Nevertheless, this dilution could lead to a lower concentration than the lowest concentration used for standard curves (0.01µM, S/N>10) or the limit of

quantification (LOQ) of the RP-UHPLC-PDA-MS system. Moreover, when using MeOH or ACN as the diluted solvent, potential solvent evaporation could happen, especially in the autosampler at 37 °C, leading to an overestimation of concentration or undetectable results when the volume of solvent is too low.

4.6. Potential solutions to reducing non-specific binding and optimization for follow-up studies

Methods for the application of Caco-2 cell permeability assay for hydrophobic compounds have already been proposed in multiple references. Even if the effect of adding 14% (*w/v*) BSA is not significant in this study, the use of BSA can still not be completely ruled out. In this research, a relatively higher concentration of BSA was used to solve the non-specific binding since the increasing percentage of BSA in the receiver could lead to higher Papp values for some drugs before reaching equilibrium (Saha & Kou, 2002). However, Cai et al. (2019) suggested that 0.5% BSA may be a better choice compared to 4% BSA with significant improvement in data quality. Therefore, the effect of adding BSA and its concentration should be investigated in further research. In addition, previous research also suggests that the addition of low concentration (~1-2%, avoid damaging the Caco-2 cells) of organic cosolvent (*e.g.* DMSO or propylene glycol) to the donor compartment could help increase the solubility (Awortwe et al., 2014). Another possible solution is to use a fasted state simulated intestinal fluid (FaSSIF) medium instead of the HBSS medium in the apical chamber. This medium can provide a similar environment to human intestine (containing e.g. bile salts, phospholipids, and cholesterol) which can help reduce surface tension and form micellar structures (Klumpp et al., 2020). Fossati et al. (2008) proved that Caco-2 cell permeability assay with FaSSIF in the AP chamber and HBSS with 1% BSA in the BL chamber is a reliable method for highly lipophilic compounds. Adding hydrophilic coating which introduced negative hydroxyl, carbonyl and carboxyl groups could also help to deal with the plastic binding, especially when the compound is in negative forms as well (Schlenoff, 2014).

The loss in **Fig. 10** could also be related to the variables in sampling or quantification and a more systematic procedure of the Caco-2 cell permeability assay should be designed based on lab conditions and compound properties in the following research. An individual toxicity assay of prenylated (iso)flavonoids could be conducted to eliminate the potential influence on cell integrity and to better design the initial concentration added. To better understand the process of non-specific binding, the Caco-2 cells could be separated from AP inserts and detected at the end of the permeability assay. As for the concentration-time profile, the reaction did not reach equilibrium at 3h and the extended experiment duration could be conducted as well. In addition, the non-preventable use of plastic (e.g. pipette tips) and the compounds which were absorbed into the inner layer of the plate and difficult to be recovered should also be considered.

4.7. Conclusion

In summary, more prenylated (iso)flavonoids (around 50%) bound to the plastic plate compared with non-prenylated genistein and propranolol due to the high lipophilicity. The addition of 14% (*w/v*) BSA did not reduce this non-specific binding. The concentration-time profile of wighteone showed that rapid binding occurred at the beginning and was fastest in the first 10 min, suggesting that adsorption was the main process that happened during the non-specific binding while the absorption could last for at least 3 hours. The Papp values of lupiwighteone and wighteone were 0.24×10^{-6} and 0.27×10^{-6} cm/s. Due to this non-specific binding, the Papp values obtained could not be interpreted directly. However, it was found that the permeability of prenylated (iso)flavonoids was lower than expected and was possibly even lower than genistein since the samples still stayed in the free medium in the AP chamber rather than pass the cell monolayer. High lipophilicity, low solubility, and ionization may hinder intestinal absorption. The influence of the position of prenyl groups still needs to be investigated. In the following studies, optimized Caco-2 cell permeability assay with different mediums and concentrations of BSA could be compared to further reduce the influence of non-specific binding. This research found that high lipophilicity of prenylated (iso)flavonoids could be a main challenge in Caco-2 cell permeability assay. By modelling the sample distribution in plate, free medium and cell monolayers, it is possible to describe the absorption process better to obtain more accurate Papp values.

Acknowledgements

This thesis was completed under the careful guidance of my supervisor, **Janniek Ritsema** and **Dr. Nynke Kramer,** for their support, guidance, and encouragement throughout the entire project. During the process of experiments and writing, they always gave me insightful suggestions and feedback and helped me to do better in all aspects of my studies. I am grateful to **Jingxuan Wang** for her role in introducing and instructing me in the practical lab work in cell culturing and seeding. Thanks for your considerate instruction and for always being there to help me with the questions and discussion.

Furthermore, I would like to thank **Mathias Busch**, who organized the thesis ring 3 and gave us constructive opinions on the writing in an attractive way. I would also like to show my sincere appreciation to other technicians and lab assistants in both TOX and FCH, **Alexandros Sotiriou, Sebas Wesseling, Wouter Bakker, Edwin Bakx,** and **Naomi Versteeg** who helped me with questions and introduced me to the use of equipment.

Special thanks go to my family and friends for their patience, understanding, and encouragement. It's your support that gave me tremendous inspiration and motivation, which not only enabled me to complete my studies but also helped me to pass through all the stressful and anxious periods.

Lastly, thanks to all the participants who generously shared insights and thanks again to all my concerned, supportive, and helpful supervisors, friends, and family.

Appendix A. Detailed dilution plan of working stock solution

A.1. Dilution plan for working stock solution preparation. Working stock solutions were prepared to the same concentration (20000 µM) by adding V0 µL master stock solution to Vs µL 100% DMSO. These working stock solutions were kept in the freezer until use.

Compound	Molecular weight (g/mol)	Concentration of master stock solution (mg/ml)	Concentration of master stock solution (µM)	Concentration of working stock solution (µM)	Dilution times	Stock solution needed V0 (µL)	The volume of added solvent Vs (µL)	The final volume of working stock solution (µL)
Genistein	270.2	10	37004.1	20000	1.9X	15	12.8	27.8
Wighteone	338.4	20	59110.4	20000	3.0X	10	19.6	29.6
Lupiwighteone	338.4	10	29555.2	20000	1.5X	15	7.2	22.2
6,8-DPG	406.5	20	49204.1	20000	2.5X	10	14.6	24.6
Propranolol	259.4	10	38557.9	20000	1.9X	15	13.9	28.9

Appendix B. RP-UHPLC-PDA-MS analysis methods

B.1. Gradient used for RP-UHPLC-PDA-MS analysis

Time (min)	Segment time (min)	Flow (mL/min)	A (%)	B (%)	Required CV	Total (mL)	A (mL)	B (mL)
0.00	0.00	0.400	75	25				
1.09	1.09	0.400	75	25	1.0	0.44	0.33	0.11
14.72	13.63	0.400	25	75	12.5	5.45	1.36	4.09
15.81	1.09	0.400	0	100	1.0	0.44	0.00	0.44
21.26	5.45	0.400	0	100	5.0	2.18	0.00	2.18
22.35	1.09	0.400	75	25	1.0	0.44	0.33	0.11
27.80	5.45	0.400	75	25	5.0	2.18	1.64	0.55

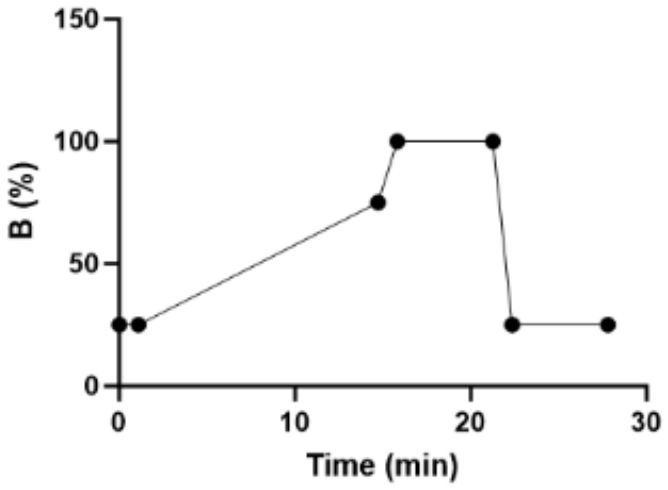

B.2. Gradient changes during RP-UHPLC-PDA-MS analysis

B.3. Retention time, m/z, and ionization mode of each compound in RP-UHPLC-PDA-MS analysis

Compound	Retention time (min)	*m/z* (Full MS)	Ionization mode
Genistein	4.95	269.2	Negative
Wighteone	10.33	337.4	Negative
Lupiwighteone	9.97	337.4	Negative
6,8-DPG	14.28	405.5	Negative
Propranolol	3.18	260.4	Positive

Appendix C. Standard curves

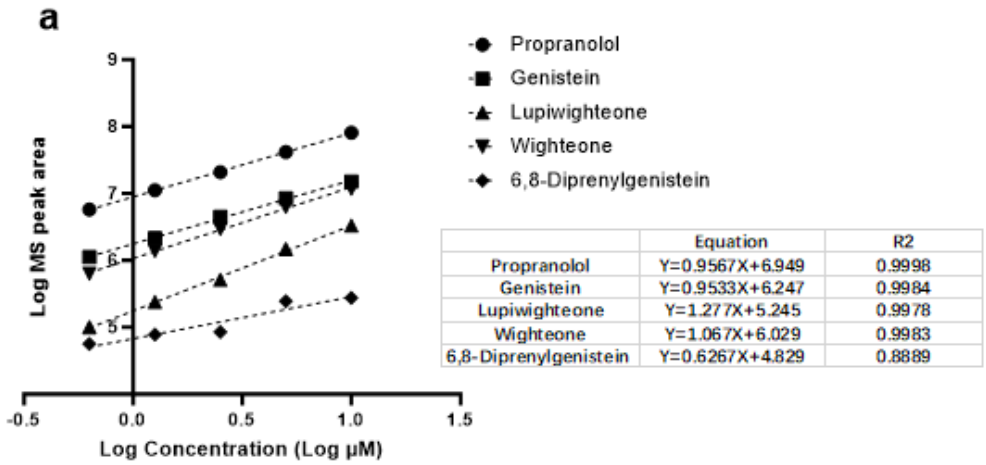

	Equation	R2
Propranolol	Y=0.9567X+6.949	0.9998
Genistein	Y=0.9533X+6.247	0.9984
Lupiwighteone	Y=1.277X+5.245	0.9978
Wighteone	Y=1.067X+6.029	0.9983
6,8-Diprenylgenistein	Y=0.6267X+4.829	0.8889

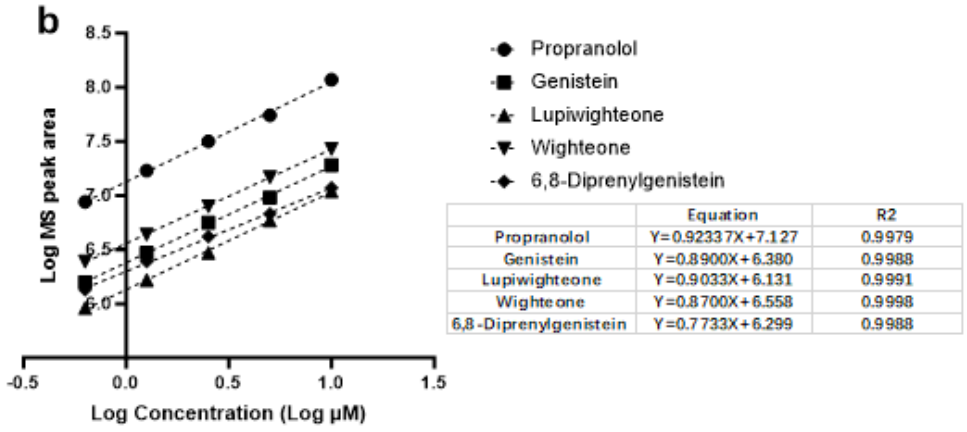

	Equation	R2
Propranolol	Y=0.9233X+7.127	0.9979
Genistein	Y=0.8900X+6.380	0.9988
Lupiwighteone	Y=0.9033X+6.131	0.9991
Wighteone	Y=0.8700X+6.558	0.9998
6,8-Diprenylgenistein	Y=0.7733X+6.299	0.9988

C.1. Standard curves for assessment of extraction efficiency and apparatus affinity without cells. a: Sample solution was diluted in 100% exposure medium; b: Sample solution was diluted in 80% MeOH and 20% exposure medium.

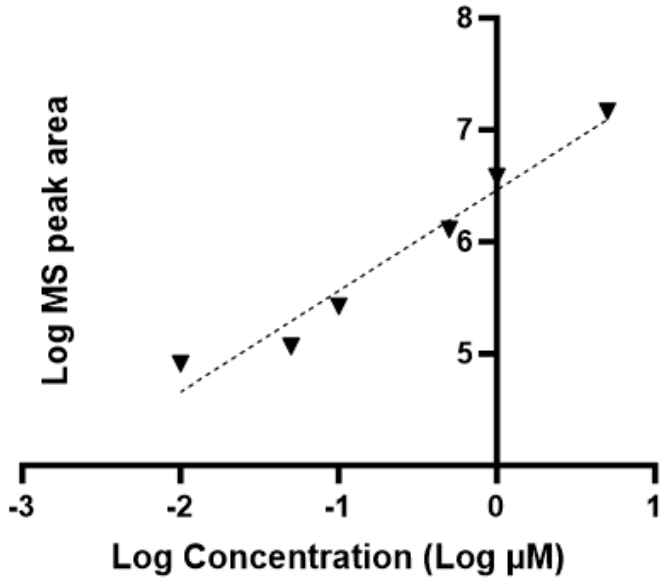

C.2. Standard curve for the concentration-time profile of wighteone in 3h permeability assay. Linear regression: $Y=0.9024X + 6.462$, $R^2 = 0.9604$.

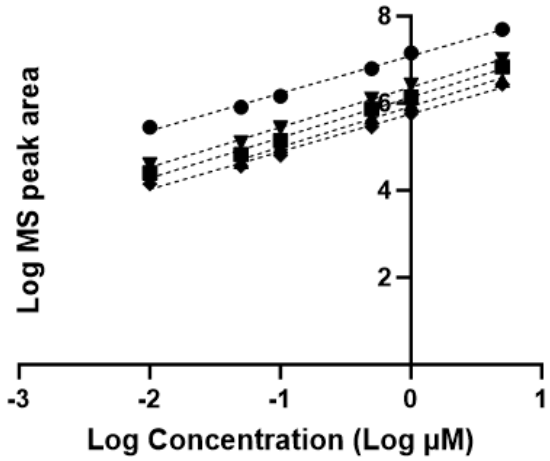

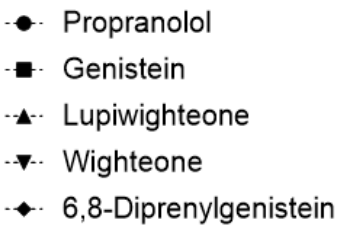

	Equation	R2
Propranolol	Y=0.8595X+7.089	0.9943
Genistein	Y=0.9303X+6.141	0.9927
Lupiwighteone	Y=0.9361X+5.929	0.9959
Wighteone	Y=0.9207X+6.371	0.9966
6,8-Diprenylgenistein	Y=0.8664X+5.757	0.9900

C.3. Standard curves for Papp value calculation in 3h Caco-2 cell permeability assay

Appendix D. Results of the assessment of evaporation

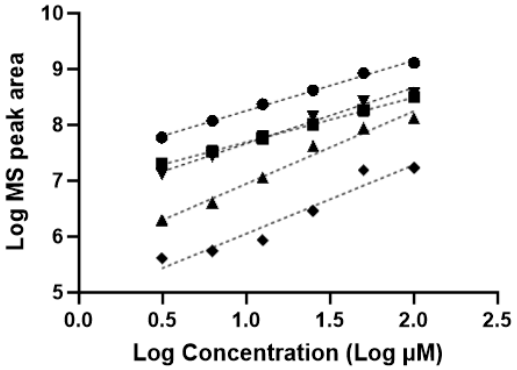

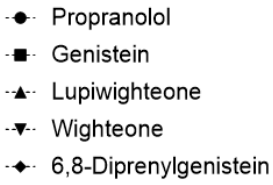

	Equation	R2
Propranolol	Y=0.9001X+7.359	0.9961
Genistein	Y=0.8013X+6.896	0.9997
Lupiwighteone	Y=1.300X+5.651	0.9804
Wighteone	Y=1.002X+6.668	0.9859
6,8-Diprenylgenistein	Y=1.231X+4.827	0.9302

D.1. Standard curves for assessment of evaporation in permeability assay without cells

D.2. MS peak area before and after evaporation and concentration changes after evaporation

Samples	Area at 280nm without evaporation in log scale (2 Log µM)	Area at 280nm after evaporation in log scale	Concentration remained after evaporation %
Propranolol	9.11	9.18	104.98
Genistein	8.50	8.51	102.90
Lupiwighteone	8.12	8.20	91.71
Wighteone	8.57	8.60	84.71
6,8-Diprenylgenistein	7.23	7.31	103.93

Appendix E. Results of 2h Caco-2 cell permeability assay

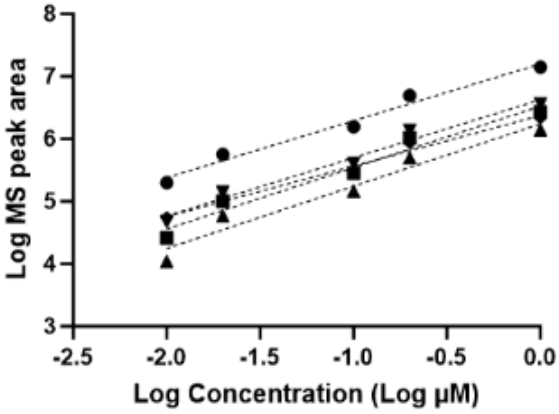

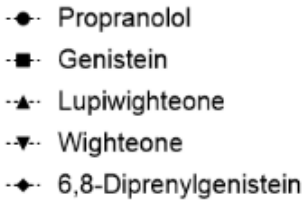

	Equation	R2
Propranolol	Y=0.9107X+7.200	0.9790
Genistein	Y=0.9828X+6.524	0.9644
Lupiwighteone	Y=0.9974X+6.240	0.9507
Wighteone	Y=0.9302X+6.627	0.9749
6,8-Diprenylgenistein	Y=0.8096X+6.375	0.9833

E.1. Standard curves for Papp value calculation in 2h Caco-2 cell permeability assay

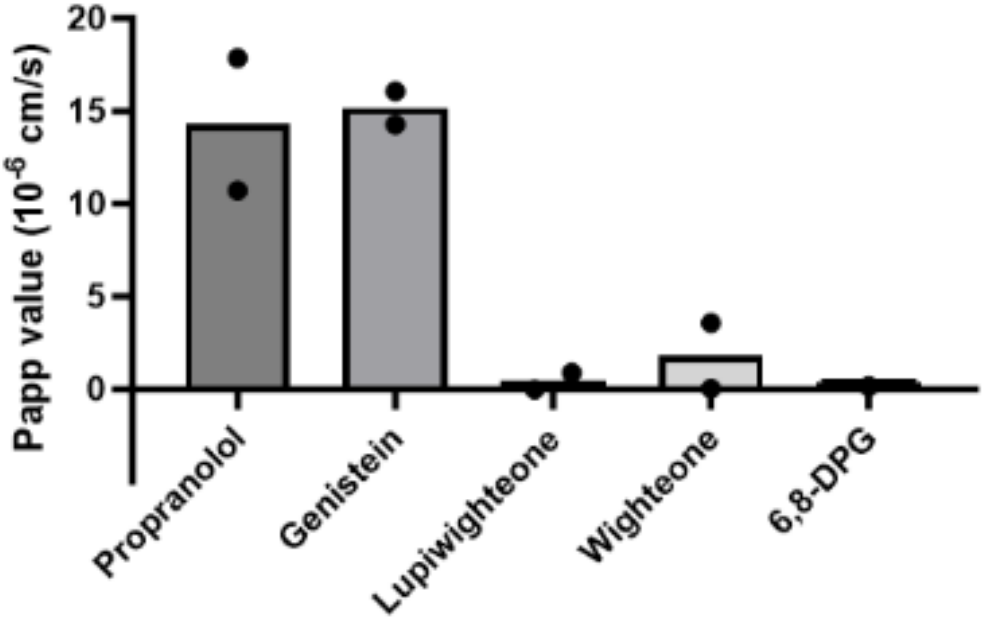

E.2. Papp values (10^{-6} cm/s) of 2h Caco-2 cell permeability assay. The initial concentration (C_0) was assumed to be 100 μM

Appendix F. Results of 4h concentration-time profile of wighteone

A 4h assessment was conducted to better describe the concentration-time profile of wighteone. Propranolol was added to each vial as an internal standard after sampling to correct the solvent evaporation. Due to the limitations in availability of equipment, samples were detected by 2 different RP-UHPLC-PDA-MS systems. A high percentage of loss (38%-53%) was observed in the results from one system which was then suspected to be less accurate. Therefore, this assay is not discussed in the main text and included in the Appendix for completeness.

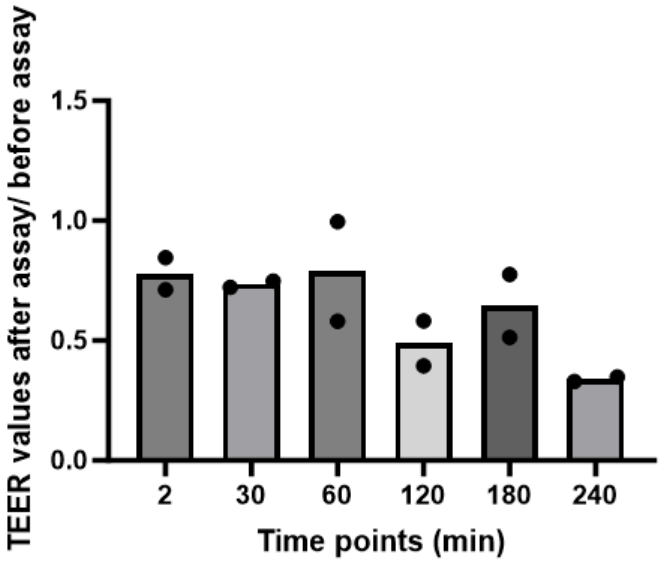

F.1. TEER value ($\Omega \cdot cm^2$) changes after 4h permeability assay for the concentration-time profile of wighteone

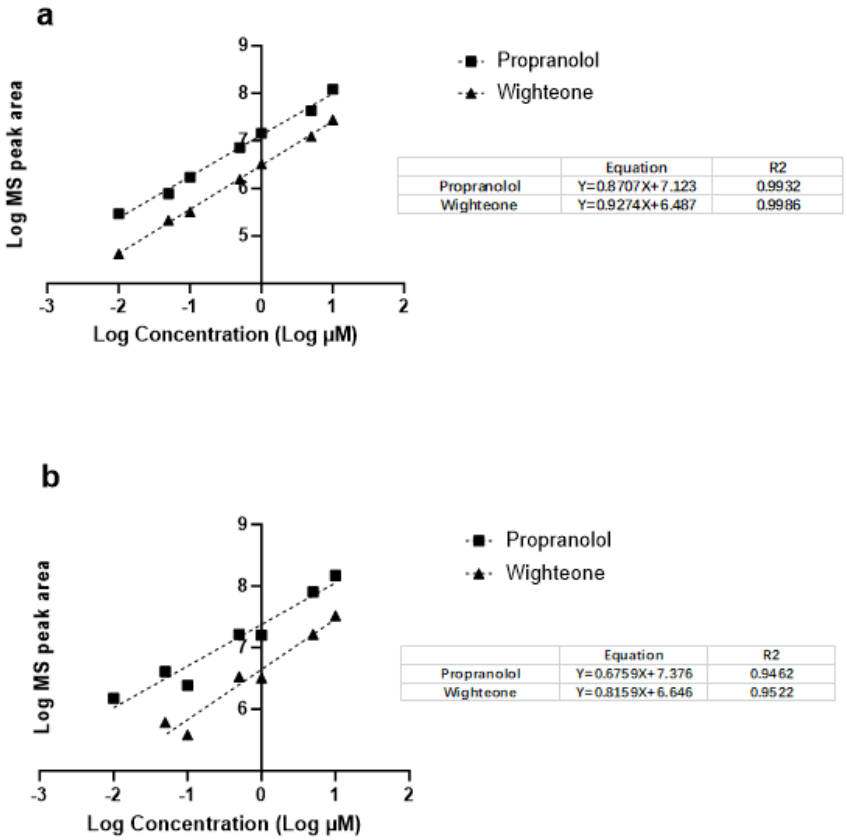

F.2. Standard curves for 4h permeability for the concentration-time profile of wighteone. a: Standard curve for the first duplicate (System 1 in the laboratory of Food Chemistry); b: Standard curve for the second duplicate (System 3 in the laboratory of Food Chemistry)

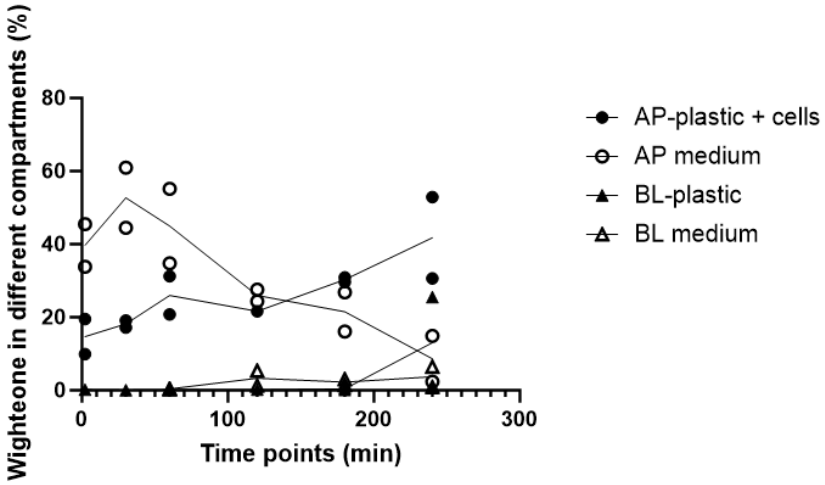

F.3. Distribution of wighteone with the time changes. AP-plastic + cells: percentage of samples bound to the insert and cells; AP medium: percentage of samples in the free medium in the AP chamber; BL-plastic: percentage of samples bind to the wells; BL medium: percentage of samples in the free medium in the BL chamber.

References

Ahmed, I., Leach, D. N., Wohlmuth, H., De Voss, J. J., & Blanchfield, J. T. (2020). Caco-2 Cell Permeability of Flavonoids and Saponins from Gynostemma pentaphyllum: the Immortal Herb. *ACS Omega*, *5*(34), 21561-21569. https://doi.org/10.1021/acsomega.0c02180

Angelis, I. D., & Turco, L. (2011). Caco-2 Cells as a Model for Intestinal Absorption. *Current Protocols in Toxicology*, *47*(1), 20.26.21-20.26.15. https://doi.org/https://doi.org/10.1002/0471140856.tx2006s47

Awortwe, C., Fasinu, P. S., & Rosenkranz, B. (2014). Application of Caco-2 cell line in herb-drug interaction studies: current approaches and challenges. *J Pharm Pharm Sci*, *17*(1), 1-19. https://doi.org/10.18433/j30k63

Bae, M. G., Hwang-Bo, J., Lee, D. Y., Lee, Y. H., & Chung, I. S. (2021). Effects of 6,8-Diprenylgenistein on VEGF-A-Induced Lymphangiogenesis and Lymph Node Metastasis in an Oral Cancer Sentinel Lymph Node Animal Model. *Int J Mol Sci*, *22*(2). https://doi.org/10.3390/ijms22020770

Barron, D., & Ibrahim, R. K. (1996). Isoprenylated flavonoids - A survey [Review]. *Phytochemistry*, *43*(5), 921-982. https://doi.org/10.1016/S0031-9422(96)00344-5

Boldon, J. A., & Shell, T. A. (2023). Physicochemical properties of acedoben and its trifluoroacetamido derivative. *Results in Chemistry*, *6*. https://doi.org/10.1016/j.rechem.2023.101075

Cai, X., Madari, S., Walker, A., Paiva, A., Li, Y., Herbst, J., Shou, W., & Weller, H. (2019). Addition of Optimized Bovine Serum Albumin Level in a High-Throughput Caco-2 Assay Enabled Accurate Permeability Assessment for Lipophilic Compounds. *SLAS Discov*, *24*(7), 738-744. https://doi.org/10.1177/2472555219848483

Chen, L., Cao, H., Huang, Q., Xiao, J., & Teng, H. (2022). Absorption, metabolism and bioavailability of flavonoids: a review. *Crit Rev Food Sci Nutr*, *62*(28), 7730-7742. https://doi.org/10.1080/10408398.2021.1917508

Chen, Y., Zhao, Y. H., Jia, X. B., & Hu, M. (2008). Intestinal absorption mechanisms of prenylated flavonoids present in the heat-processed Epimedium koreanum Nakai (Yin Yanghuo). *Pharm Res*, *25*(9), 2190-2199. https://doi.org/10.1007/s11095-008-9602-7

Chen, Z., Zheng, S., Li, L., & Jiang, H. (2014). Metabolism of flavonoids in human: a comprehensive review. *Curr Drug Metab*, *15*(1), 48-61. https://doi.org/10.2174/1389200215011402181250 20

Chillistone, S., & Hardman, J. G. (2017). Factors affecting drug absorption and distribution. *Anaesthesia & Intensive Care Medicine*, *18*(7), 335-339. https://doi.org/10.1016/j.mpaic.2017.04.007

Choi, H., Park, J.-S., Kim, K.-M., Kim, M., Ko, K.-W., Hyun, C.-G., Ahn, J. W., Seo, J.-H., & Kim, S.-Y. (2018). Enhancing the antimicrobial effect of genistein by biotransformation in microbial system. *Journal of Industrial and Engineering Chemistry*, *63*, 255-261. https://doi.org/10.1016/j.jiec.2018.02.023

D'Almeida, R. E., Torres Carro, R., Simonetta, S., Zampini, I. C., Simirgiotis, M., Borquez, J., Isla, M. I., & Alberto, M. R. (2020). Flavonoid-enriched fractions from Parastrephia lucida: Phytochemical, anti-inflammatory, antioxidant characterizations, and analysis of their toxicity. *South African Journal of Botany*, *135*, 465-475. https://doi.org/10.1016/j.sajb.2020.09.019

Daruhazi, A. E., Kiss, T., Vecsernyes, M., Szente, L., Szoke, E., & Lemberkovics, E. (2013). Investigation of transport of genistein, daidzein and their inclusion complexes prepared with different cyclodextrins on Caco-2 cell line. *J Pharm Biomed Anal*, *84*, 112-116. https://doi.org/10.1016/j.jpba.2013.05.012

Day, A. J., Cañada, F. J., Díaz, J. C., Kroon, P. A., McLauchlan, R., Faulds, C. B., Plumb, G. W., Morgan, M. R. A., & Williamson, G. (2000). Dietary flavonoid and isoflavone glycosides are hydrolysed by the lactase site of lactase phlorizin hydrolase. *FEBS Letters*, *468*(2), 166-170. https://doi.org/https://doi.org/10.1016/S0014-5793(00)01211-4

de Oliveira, A. M., de Freitas, A. F. S., Costa, W. K., Machado, J. C. B., Bezerra, I. C. F., Ferreira, M. R. A., Paiva, P. M. G., Napoleão, T. H., & Soares, L. A. L. (2022). Flavonoid-rich fraction of Croton blanchetianus Baill. (Euphorbiaceae) leaves: Chemical profile, acute and subacute toxicities, genotoxicity and antioxidant potential. *South African Journal of Botany*, *144*, 238-249. https://doi.org/10.1016/j.sajb.2021.08.040

de Souza, M. C., de Souza Mesquita, L. M., Pena, F. L., Tamborlin, L., da Silva, L. C., Viganó, J., Antunes, A. E. C., Luchessi, A. D., Duarte, M. C. T., Barbero, G. F., & Rostagno, M. A. (2022). Potential application for antimicrobial and antileukemic therapy of a flavonoid-rich fraction of Camellia sinensis. *Food Chemistry Advances*, *1*. https://doi.org/10.1016/j.focha.2022.100042

Ding, R., Jian, Y., Kan, H., Liu, Z.-Y., Liu, S., Liu, Z.-Q., & Zhou, J. (2016). Studies on the intestinal absorption

of the alkaloids in the Gancaofuzi decoction in a Caco-2 cell culture system by UPLC–MS/MS analysis. *Chinese Chemical Letters*, *27*(6), 915-919. https://doi.org/10.1016/j.cclet.2016.03.001

Drennen, C., Gorse, E., & Stratford, R. E., Jr. (2018). Cellular Pharmacokinetic Model-Based Analysis of Genistein, Glyceollin, and MK-571 Effects on 5 (and 6)-Carboxy-2',7'-Dichloroflourescein Disposition in Caco-2 Cells. *J Pharm Sci*, *107*(4), 1194-1203. https://doi.org/10.1016/j.xphs.2017.12.004

Dupire, C., Chennell, P., Pereira, B., Courtiol, N., Buj, S., Cueff, R., Crauste-Manciet, S., Sautou, V., & Morgat, C. (2023). A proof of principle study using radiopharmaceuticals to quantify and localize container-content interactions in medical syringes. *Sci Rep*, *13*(1), 2721. https://doi.org/10.1038/s41598-023-29923-z

Fossati, L., Dechaume, R., Hardillier, E., Chevillon, D., Prevost, C., Bolze, S., & Maubon, N. (2008). Use of simulated intestinal fluid for Caco-2 permeability assay of lipophilic drugs. *International Journal of Pharmaceutics*, *360*(1-2), 148-155. https://doi.org/10.1016/j.ijpharm.2008.04.034

Fukazawa, T., Yamazaki, Y., & Miyamoto, Y. (2010). Reduction of non-specific adsorption of drugs to plastic containers used in bioassays or analyses. *J Pharmacol Toxicol Methods*, *61*(3), 329-333. https://doi.org/10.1016/j.vascn.2009.12.005

Han, R. M., Tian, Y. X., Liu, Y., Chen, C. H., Ai, X. C., Zhang, J. P., & Skibsted, L. H. (2009). Comparison of flavonoids and isoflavonoids as antioxidants. *J Agric Food Chem*, *57*(9), 3780-3785. https://doi.org/10.1021/jf803850p

Illum, L., & Bundgaard, H. (1982). Sorption of drugs by plastic infusion bags. *International Journal of Pharmaceutics*, *10*(4), 339-351. https://doi.org/https://doi.org/10.1016/0378-5173(82)90168-5

Kalli, S., Araya-Cloutier, C., Chapman, J., Sanders, J.-W., & Vincken, J.-P. (2022). Prenylated (iso)flavonoids as antifungal agents against the food spoiler Zygosaccharomyces parabailii. *Food Control*, *132*. https://doi.org/10.1016/j.foodcont.2021.108434

Kalli, S., Araya-Cloutier, C., Hageman, J., & Vincken, J.-P. (2021). Insights into the molecular properties underlying antibacterial activity of prenylated (iso)flavonoids against MRSA. *Scientific Reports*, *11*(1), 14180. https://doi.org/10.1038/s41598-021-92964-9

Katneni, K., Pham, T., Saunders, J., Chen, G., Patil, R., White, K. L., Abla, N., Chiu, F. C. K., Shackleford, D. M., & Charman, S. A. (2018). Using Human Plasma as an Assay Medium in Caco-2 Studies Improves Mass Balance for Lipophilic Compounds. *Pharm Res*, *35*(11), 210. https://doi.org/10.1007/s11095-018-2493-3

Klumpp, L., Leigh, M., & Dressman, J. (2020). Dissolution behavior of various drugs in different FaSSIF versions. *Eur J Pharm Sci*, *142*, 105138. https://doi.org/10.1016/j.ejps.2019.105138

Krishna, G., Chen, K.-j., Lin, C.-c., & Nomeir, A. A. (2001). Permeability of lipophilic compounds in drug discovery using in-vitro human absorption model, Caco-2. *International Journal of Pharmaceutics*, *222*(1), 77-89. https://doi.org/https://doi.org/10.1016/S0378-5173(01)00698-6

Kus, M., Ibragimow, I., & Piotrowska-Kempisty, H. (2023). Caco-2 Cell Line Standardization with Pharmaceutical Requirements and In Vitro Model Suitability for Permeability Assays. *Pharmaceutics*, *15*(11). https://doi.org/10.3390/pharmaceutics15112523

Lindsley, C. W. (2014). Lipophilicity. In *Encyclopedia of Psychopharmacology* (pp. 1-6). https://doi.org/10.1007/978-3-642-27772-6_7015-1

Liu, Y. P., Yu, X. M., Zhang, W., Wang, T., Jiang, B., Tang, H. X., Su, Q. T., & Fu, Y. H. (2020). Prenylated chromones and flavonoids from Artocarpus heterophyllus with their potential antiproliferative and anti-inflammatory activities. *Bioorg Chem*, *101*, 104030. https://doi.org/10.1016/j.bioorg.2020.104030

Lv, H. W., Wang, Q. L., Luo, M., Zhu, M. D., Liang, H. M., Li, W. J., Cai, H., Zhou, Z. B., Wang, H., Tong, S. Q., & Li, X. N. (2023). Phytochemistry and pharmacology of natural prenylated flavonoids. *Arch Pharm Res*, *46*(4), 207-272. https://doi.org/10.1007/s12272-023-01443-4

Ma, E. Z., & Khachemoune, A. (2023). Flavonoids and their therapeutic applications in skin diseases. *Arch Dermatol Res*, *315*(3), 321-331. https://doi.org/10.1007/s00403-022-02395-3

Magni, G., Riboldi, B., Petroni, K., & Ceruti, S. (2022). Flavonoids bridging the gut and the brain: Intestinal metabolic fate, and direct or indirect effects of natural supporters against neuroinflammation and neurodegeneration. *Biochem Pharmacol*, *205*, 115257. https://doi.org/10.1016/j.bcp.2022.115257

Marino, A. M., Yarde, M., Patel, H., Chong, S., & Balimane, P. V. (2005). Validation of the 96 well Caco-2 cell culture model for high throughput permeability assessment of discovery compounds. *Int J Pharm*, *297*(1-2), 235-241. https://doi.org/10.1016/j.ijpharm.2005.03.008

Murota, K., Nakamura, Y., & Uehara, M. (2018). Flavonoid metabolism: the interaction of metabolites and gut

microbiota. *Biosci Biotechnol Biochem*, *82*(4), 600-610. https://doi.org/10.1080/09168451.2018.1444467

Osorio, M., Carvajal, M., Vergara, A., Butassi, E., Zacchino, S., Mascayano, C., Montoya, M., Mejias, S., Martin, M. C., & Vasquez-Martinez, Y. (2021). Prenylated Flavonoids with Potential Antimicrobial Activity: Synthesis, Biological Activity, and In Silico Study. *Int J Mol Sci*, *22*(11). https://doi.org/10.3390/ijms22115472

Palmgren, J. J., Monkkonen, J., Korjamo, T., Hassinen, A., & Auriola, S. (2006). Drug adsorption to plastic containers and retention of drugs in cultured cells under in vitro conditions. *Eur J Pharm Biopharm*, *64*(3), 369-378. https://doi.org/10.1016/j.ejpb.2006.06.005

Panche, A. N., Diwan, A. D., & Chandra, S. R. (2016). Flavonoids: an overview. *J Nutr Sci*, *5*, e47. https://doi.org/10.1017/jns.2016.41

Papadopoulou, A., Green, R. J., & Frazier, R. A. (2005). Interaction of Flavonoids with Bovine Serum Albumin: A Fluorescence Quenching Study. *Journal of Agricultural and Food Chemistry*, *53*(1), 158-163. https://doi.org/10.1021/jf048693g

Ravikanth, P. V., & Ramanamurthy, K. V. (2018). Permeability assessment of drug substances using in vitro and ex vivo screening techniques.

Safe, S., Jayaraman, A., Chapkin, R. S., Howard, M., Mohankumar, K., & Shrestha, R. (2021). Flavonoids: structure-function and mechanisms of action and opportunities for drug development. *Toxicol Res*, *37*(2), 147-162. https://doi.org/10.1007/s43188-020-00080-z

Saha, P., & Kou, J. H. (2002). Effect of bovine serum albumin on drug permeability estimation across Caco-2 monolayers. *European Journal of Pharmaceutics and Biopharmaceutics*, *54*(3), 319-324. https://doi.org/https://doi.org/10.1016/S0939-6411(02)00089-9

Schlenoff, J. B. (2014). Zwitteration: coating surfaces with zwitterionic functionality to reduce nonspecific adsorption. *Langmuir*, *30*(32), 9625-9636. https://doi.org/10.1021/la500057j

Shen, N., Wang, T., Gan, Q., Liu, S., Wang, L., & Jin, B. (2022). Plant flavonoids: Classification, distribution, biosynthesis, and antioxidant activity. *Food Chem*, *383*, 132531. https://doi.org/10.1016/j.foodchem.2022.132531

Shi, S., Li, J., Zhao, X., Liu, Q., & Song, S. J. (2021). A comprehensive review: Biological activity, modification and synthetic methodologies of prenylated flavonoids. *Phytochemistry*, *191*, 112895. https://doi.org/10.1016/j.phytochem.2021.112895

Singh, P., Sharma, S., & Rath, S. K. (2022). A versatile flavonoid Quercetin: Study of its toxicity and differential gene expression in the liver of mice. *Phytomedicine Plus*, *2*(1). https://doi.org/10.1016/j.phyplu.2021.100148

Spencer, J. P. (2003). Metabolism of tea flavonoids in the gastrointestinal tract. *J Nutr*, *133*(10), 3255S-3261S. https://doi.org/10.1093/jn/133.10.3255S

Tang, H., Huang, L., Zhao, D., Sun, C., & Song, P. (2020). Interaction mechanism of flavonoids on bovine serum albumin: Insights from molecular property-binding affinity relationship. *Spectrochim Acta A Mol Biomol Spectrosc*, *239*, 118519. https://doi.org/10.1016/j.saa.2020.118519

Tao, Z., Liu, J., Jiang, Y., Gong, L., & Yang, B. (2017). Synthesis of prenylated flavonols and their potents as estrogen receptor modulator. *Sci Rep*, *7*(1), 12445. https://doi.org/10.1038/s41598-017-12640-9

Terao, J., & Mukai, R. (2014). Prenylation modulates the bioavailability and bioaccumulation of dietary flavonoids. *Arch Biochem Biophys*, *559*, 12-16. https://doi.org/10.1016/j.abb.2014.04.002

Thilakarathna, S. H., & Rupasinghe, H. P. (2013). Flavonoid bioavailability and attempts for bioavailability enhancement. *Nutrients*, *5*(9), 3367-3387. https://doi.org/10.3390/nu5093367

Tronina, T., Bartmanska, A., Poplonski, J., Rychlicka, M., Sordon, S., Filip-Psurska, B., Milczarek, M., Wietrzyk, J., & Huszcza, E. (2023). Prenylated Flavonoids with Selective Toxicity against Human Cancers. *Int J Mol Sci*, *24*(8). https://doi.org/10.3390/ijms24087408

van Dinteren, S., Araya-Cloutier, C., de Bruijn, W. J. C., & Vincken, J. P. (2021). A targeted prenylation analysis by a combination of IT-MS and HR-MS: Identification of prenyl number, configuration, and position in different subclasses of (iso)flavonoids. *Anal Chim Acta*, *1180*, 338874. https://doi.org/10.1016/j.aca.2021.338874

van Dinteren, S., Meijerink, J., Witkamp, R., van Ieperen, B., Vincken, J. P., & Araya-Cloutier, C. (2022). Valorisation of liquorice (Glycyrrhiza) roots: antimicrobial activity and cytotoxicity of prenylated (iso)flavonoids and chalcones from liquorice spent (G. glabra, G. inflata, and G. uralensis). *Food Funct*, *13*(23), 12105-12120. https://doi.org/10.1039/d2fo02197h

Vongdeth, K., Ran, L., Yan, L., & Wang, Q. (2018). Synthesis and Activity Evaluation of Novel Prenylated Flavonoids as Antiproliferative Agents. *Chemical Research in Chinese Universities*, *34*(4), 564-570. https://doi.org/10.1007/s40242-018-8013-5

Wen, L., Shi, D., Zhou, T., Tu, J., He, M., Jiang, Y., & Yang, B. (2020). Identification of two novel prenylated flavonoids in mulberry leaf and their bioactivities. *Food Chem*, *315*, 126236. https://doi.org/10.1016/j.foodchem.2020.126236

Xu, M.-J., Wu, B., Ding, T., Chu, J.-H., Li, C.-Y., Zhang, J., Wu, T., Wu, J., Liu, S.-J., Liu, S.-L., Ju, W.-Z., & Li, P. (2012). Simultaneous characterization of prenylated flavonoids and isoflavonoids in Psoralea corylifolia L. by liquid chromatography with diode-array detection and quadrupole time-of-flight mass spectrometry. *Rapid Communications in Mass Spectrometry*, *26*(19), 2343-2358. https://doi.org/https://doi.org/10.1002/rcm.6361

Yamada, N., Negoro, R., Watanabe, K., & Fujita, T. (2023). Generation of Caco-2 cells with predictable metabolism by CYP3A4, UGT1A1 and CES using the PITCh system. *Drug Metab Pharmacokinet*, *50*, 100497. https://doi.org/10.1016/j.dmpk.2023.100497

Yang, X., Jiang, Y., Yang, J., He, J., Sun, J., Chen, F., Zhang, M., & Yang, B. (2015). Prenylated flavonoids, promising nutraceuticals with impressive biological activities. *Trends in Food Science & Technology*, *44*(1), 93-104. https://doi.org/10.1016/j.tifs.2015.03.007

Yang, Z., Kulkarni, K., Zhu, W., & Hu, M. (2012). Bioavailability and pharmacokinetics of genistein: mechanistic studies on its ADME. *Anticancer Agents Med Chem*, *12*(10), 1264-1280. https://doi.org/10.2174/187152012803833107

Zulfiqar, F., Khan, S. I., Ross, S. A., Ali, Z., & Khan, I. A. (2017). Prenylated flavonol glycosides from Epimedium grandiflorum: Cytotoxicity and evaluation against inflammation and metabolic disorder. *Phytochemistry Letters*, *20*, 160-167. https://doi.org/10.1016/j.phytol.2017.04.027